Supplemental data

The innate immune receptor TREM-1 promotes liver injury and fibrosis

Anh Thu Nguyen-Lefebvre, Ashwin Ajith, Vera Portik-Dobos, Daniel David Horuzsko, Ali Syed Arbab, Amiran Dzutsev, Ramses Sadek, Giorgio Trinchieri, Anatolij Horuzsko

Table of content

Supplemental methods

Mice and fibrosis induction

The generation of mice deficient in *Trem1* (on a C57BL/6J genetic background) has been described previously (17). Originally, *Trem1*$^{+/-}$ parents were bred to produce Trem1$^{-/-}$ and WT offspring. The ratio of *Trem1*$^{-/-}$, *Trem1*$^{+/-}$, and WT offspring did not deviate significantly from the expected 1:2:1 ratio. *Trem1*$^{-/-}$ and *Trem1*$^{+/-}$ animals were grossly normal, with normal body weight and appearance. WT littermate controls have been used for the liver fibrosis studies. In addition to the WT littermates, a WT littermate line or WT C57BL/6J mice, bred in our facility, have been used as WT controls for the experiments. The expression of *Trem1* was analyzed using forward primer (5'-CGCCTGGTGGTGACCAAGGG-3') and reverse primer (5'-ACAACCGCAGTGGGCTTGGG-3') to amplify the 152-bp product. All mice were housed in a specific pathogen-free environment in the Augusta University animal facilities, and the Institutional Animal Care and Use Committee approved all animal procedures. 8-week-old male *Trem1*$^{-/-}$ or WT mice were injected with one dose of corn oil (control) or CCl_4 (2 µl/g, diluted 1:4 in corn oil) (Sigma-Aldrich, St. Louis, MO, USA) and sacrificed at 6 h, 12 h or 72 h post-treatment. Another group of *Trem1*$^{-/-}$ or WT mice were treated with corn oil (control) or CCl_4 (2 µl/g, diluted 1:4 in corn oil) twice per week over a 6-week period and then sacrificed.

Measurement of hepatic collagen deposition and cell infiltration

Mice were sacrificed and their livers removed at different time-points after CCl_4 treatment. Fibrotic nodules were visible on WT mice treated for 6 weeks with CCl_4. Liver tissues were fixed in 4% paraformaldehyde for 10 days and embedded with paraffin. 7 µm-sections were stained with NovaUltra™ Sirius Red Stain Kit (IHC World, Woodstock, MD, USA) to detect collagen deposition according to the manufacturer's recommendations. To determine cell infiltration, 7 µm sections were stained with H & E (Thermo Fisher Scientific, Waltham, MA, USA). All images

were visualized using a Zeiss Axio Imager M1 (Carl Zeiss, Oberkochen, Germany) microscope. Sirius red-positive and cell infiltration areas were measured in at least five fields (at x10 and x20 magnification) on each slide and were quantified using Image J (NIH) software.

Immunofluorescence (IF) and immunohistochemistry (IHC) staining

At different time-points after CCl_4 treatment, mice were sacrificed and their livers removed. Liver tissues were fixed in 4% paraformaldehyde for 10 days and embedded with paraffin. 7 µm sections were boiled in citrate buffer antigen retrieval solution containing 10 mM sodium citrate and 0.05% Tween-20 (both from Thermo Fisher Scientific) for 30 min and then washed twice with PBS. Liver sections were blocked in 3% bovine serum albumin (Thermo Fisher Scientific) / 5% (for IHC) or 10% (for IF) horse serum (Jackson ImmunoResearch Laboratories, Inc., West Grove, PA, USA) in PBST (PBS + 0.01% Tween 20) for 1 h before incubating with primary antibodies. For IF staining, incubation was performed in the presence of FITC-conjugated rat anti-mouse F4/80 antibody (Biolegend, San Diego, CA, USA) (#123108, clone BM8, 1:2000), PE-conjugated rat anti-mouse TREM-1 antibody (R&D Systems Inc., Minneapolis, MN, USA) (#FAB1187P, clone 174031, 1:2000), phycoerythrin (PE)- (Biolegend) (#400507, 1:2000) or FITC- (Biolegend) (#400505, 1:2000) conjugated rat IgG2a, κ isotype control antibody for 1 h at room temperature in a dark humid chamber. Sections were then washed twice with PBS, and nuclei were visualized by mounting the sections in medium containing DAPI (Vector Laboratories, Burlingame, CA, USA). For IHC staining, incubation was performed in the presence of anti-α-smooth muscle actin (α-SMA) antibody (eBioscience, San Diego, CA, USA) (#14-9760-82, clone 1A4, 1:125) for 90 min at room temperature. Sections were washed in PBS and incubated with UltraVision Quanto Detection System HRP (Thermo Fisher Scientific) according to the manufacturer's recommendations. Nuclei were visualized in the sections by counterstaining with hematoxylin. All images were visualized using Zeiss Axio Imager M1 microscope and analyzed using Axiovision SE64 (Carl Zeiss) and Image J software.

Fluorescent multiplexed immunohistochemistry assay, imaging and quantitation

Liver tissue specimens were deparaffinized for multiplexed staining using the Opal protocol. Paraffin-embedded liver tissue specimens were heated at 57°C overnight, residual paraffin was removed using xylene, and tissues were rehydrated in a series of graded alcohols to distilled water. Antigen retrieval was performed according to the manufacturer's protocol (Perkin Elmer, Waltham, MA, USA). Following cooling and washing with TBST, tissue sections were blocked by 30 min incubation with 10% normal goat serum (Jackson Immunoresearch, #005-000-121). Tissue sections were then incubated for 1 h with primary antibody, followed by Opal polymer HRP Ms + Rb (as secondary antibody) incubation. Tissue sections were washed and the tyramide signal amplification (TSA)-dye (Opal 7-Color Manual IHC Kit, Perkin Elmer, Waltham, MA, USA) was applied. The process was repeated for staining with all primary antibodies staining: CD11b (Novus Biological, #NB11089474, 1:500), CD68 (1:1000), TREM-1 (MACs/ Miltenyi, #130-101-040, 1:200) and α-SMA (Ebioscience/ThermoFisher, #14-9760-82, 1:500). Nuclei were stained with ProLong™ Gold antifade reagent with DAPI (Invitrogen, #P36931). Multiplexed imaging analysis was performed with Opal 7-Color Manual IHC Kit (#NEL811001KT), and sections imaged at x20 on the Vectra Automated Quantitative Pathology Imaging System. Quantitation of chromogenic, fluorescent signals and percent of positive/negative cells for each marker was performed by using InForm software (version 2.3.0) (all from Perkin Elmer, Waltham, MA, USA).

Isolation of bone marrow cells, liver non-parenchymal cells, and Kupffer cells

Bone marrow cells were isolated from mouse femurs by flushing cells with PBS. Cells were then filtered through a 70 µm cell strainer (Thermo Fisher Scientific) and washed with PBS at 450*g* for 5 min at 4°C. The cell pellet was resuspended with 300 µl of ACK Lysis buffer (Thermo Fisher Scientific) and washed once with PBS before being analyzed by flow cytometry. Kupffer

cells were isolated by collagenase type I (Worthington, Lakewood, NJ, USA) digestion in vivo and in vitro, HISTOPAQUE®-1083 (Sigma Aldrich) density gradient centrifugation and MACS magnetic bead separation (Miltenyi Biotec, San Diego, CA, USA) as follows. Livers were perfused with calcium and magnesium-free 40°C prewarmed HBSS solution (Corning Life Sciences, Corning, NY, USA) and digested with collagenase type I. The cell suspension was filtered through a 70 μm cell strainer and then centrifuged at 50*g* for 5 min at 4°C to eliminate hepatocytes. Cells remaining in the supernatant were layered on HISTOPAQUE®-1083 and centrifuged at 1000*g* for 15 min at 4°C without a brake. The non-parenchymal cell fraction was washed once with PBS at 300*g* for 10 min at 4°C. Kupffer cells were isolated from the non-parenchymal cell fraction using (i) APC-conjugated rat anti-mouse CD11b (Biolegend) (#101212, clone M1/70, 1:100) and anti-APC magnetic beads (Miltenyi Biotec) (#130-090-855) and then (ii) the depleted CD11b fraction was stained with APC-conjugated rat anti-mouse F4/80 antibody (Biolegend) (#123116, clone BM8, 1:100) and anti-APC magnetic beads (Miltenyi Biotec) (#130-090-855).

Isolation of hepatic stellate cells (HSCs)

HSCs were isolated from WT and *Trem1*$^{-/-}$ mice treated with oil (control) or with CCl_4 for a 6-week period by a two-step collagenase-pronase in vivo perfusion and a one-step collagenase-pronase in vitro digestion, followed by Nycodenz® two-layer discontinuous density gradient centrifugation as described (21). Briefly, mouse livers were perfused in vivo with 42°C prewarmed EGTA buffer for 2 min, followed by 42°C prewarmed pronase E buffer (14 mg/35 ml of enzyme solution/mouse) for 5 min and finally with 42°C prewarmed collagenase type I buffer (3.7 U/40 ml of enzyme buffer/mouse). Both enzymes came from Worthington. Perfused livers were removed from the mouse rib cage and were in vitro digested in collagenase-pronase buffer containing 25 mg of pronase and 4.4 U of collagenase dissolved in 50 ml of enzyme buffer, at 40°C for 25 min. The liver cell suspension was filtered through a 70 μm cell strainer, and cells

were washed twice with cold GBSS/B buffer at 580*g* for 10 min at 4°C. The cell pellet was resuspended with 32 ml of GBSS/B and 16 mL of Nycodenz® solution (4.94 g of Nycodenz® (AXIS-SHIELD PoC AS, Oslo, Norway) in 17 mL of GBSS/A buffer). 12 mL aliquots of cell-Nycodenz® suspension were distributed into 15 ml tubes and overlaid by 1.5 ml of GBSS/B buffer. The cell suspension was centrifuged at 1,380*g* for 17 min at 4°C without a brake. HSCs were visible as a thin interface layer at the end of the centrifugation. HSCs were washed with GBSS/B buffer and seeded with DMEM (Corning) containing 10% FBS (Atlanta Biological, Flowery Branch, GA, USA) in Petri dishes for morphological analysis by microscopy. Freshly isolated HSCs were visualized using phase-contrast microscopy and fluorescence microscopy to detect retinoid fluorescence (with a DAPI filter).

Antibodies and flow cytometry analysis

Cells from bone marrow, blood and non-parenchymal cells from mouse liver were isolated and labeled with the following antibodies at 4°C for 45 minutes in the dark: F4/80 (#123108, clone BM8, 1:300), CD11b (#101212, clone M1/70, 1:300), Ly-6G (#127608, clone 1A8, 1:200), Ly-6C (#128008, clone HK1.4, 1:200), TNF-α (#506305, clone MP6-XT22, 1:300), TGF-β1 (#141403, clone TW7-16B4, 1:300) and CX3CR1 (#149005, clone SA011F11, 1:300) (all from Biolegend), IL-1b Pro-form (eBioscience) (#12-7114-80, clone NJTEN3, 1:300), TREM-1 (#FAB1187P, clone 174031, 1:300) and CCR2 (#FAB5535P, clone NJTEN3, 1: 300) (both from R&D Systems Inc.). All samples were pre-incubated with TruStain fcX (#101320, clone 93, 1:100) (Biolegend) for blocking the Fc receptors. Intracellular staining was carried out as per the manufacturer's instruction described in the True Nuclear Transcription Factor Kit (Biolegend). All experiments made use of the following isotypes as controls and were incubated with the sample at 4°C for 45 minutes in the dark: PE Rat IgG2B κ (#400608, clone RTK4530, 1:300), PE Rat IgG2a κ (#400507, clone RTK2758, 1:200), PE Rat IgG2c κ (#400707, clone RTK4174, 1:300), FITC Rat IgG2a κ (# 400505, clone RTK2758, 1: 300) and APC Rat IgG2b κ (# 400611, clone RTK4530,

1:300) (all from Biolegend), PE Rat IgG1 (Becton Dickinson) (#20615A, 1:300), PE Mouse IgG2a κ (#12-4724-73, clone eBM2a, 1:300) and PE Mouse IgG1 κ (#12-4714-81, clone P3.6.2.8.1, 1:300) (both from eBioscience). Samples were acquired on a FACSCanto (BD Biosciences) and analyzed using FlowJo software (FlowJo LLC, Ashland, Oregon, USA). Dead cells were excluded from analysis based on the forward and side scatter characteristics. For numerical representation of fluorescence intensity, the geometric mean of the corresponding fluorochrome was used.

Reverse transcription PCR and real time quantitative PCR

RNA was isolated from whole livers and purified hepatocytes, Kupffer cells, and HSCs of WT and *Trem1*$^{-/-}$ mice with TRIzol® Reagent (Ambion, Life Technology, Carlsbad, CA, USA) according to the manufacturer's recommendations. 1 µg of total RNA was treated with DNAse and reverse transcribed with the RT^2 First Strand Kit (Qiagen, Valencia, CA, USA) according to the manufacturer's recommendations. PCR for *Trem1* and *Actb* was performed with a Bio-Rad T1000™ Thermal Cycler machine at 95°C (3 min) followed by 40 cycles of 95°C (15 sec), 64°C (45 sec) for *Trem1* and 61°C (45 sec) for *Actb*. Real time quantitative PCR was performed for 40 cycles of 20 sec at 95°C and 30 sec at different temperatures for an annealing/extension step using an ABI StepOnePlus™ detection system (Applied Biosystems, Foster City, CA, USA). Specific primer sequences and the expected product sizes are listed in Supplemental Table 1. Quantification was performed by normalizing the Ct values of each sample to rRNA 18S, *Actb*, *Gapdh* and *Hprt1*. The global quantification for each gene was based on the published mathematical formula (Suppl. Ref.1). Values are expressed as fold induction in comparison to oil-treated mice. Purified Kupffer cells from WT mice and *Trem1*$^{-/-}$ mice treated with CCl_4 for 6 h (n=3 mice/group) and 12 h (n=3 mice/group) were pooled because of the low number of Kupffer cells per mouse. Total RNA isolated from these Kupffer cells was reverse transcribed as described above.

RNA sequencing and data analysis

Total RNA from Kupffer cells was extracted using TRIzol® (Thermo Fisher Scientific) according to the manufacturer's instructions. An RNA-seq library was prepared using Lexogen QuantSeq 3' mRNA-Seq Library Prep Kit for Illumina (#015.96) according to the manufacturer's protocol. The resultant library was sequenced on Illumina NextSeq 500 using 75 cycles High Output Kit v2 (#FC-404-2005). Bcl files were converted to fastq files on Basespace (Illumina) and were further processed on NIH Biowulf computer cluster. Briefly, sequences were preprocessed using Trimmomatic (Suppl. Ref.2) and aligned to the mouse genome (mm10 annotation), and reads per gene/feature were counted using STAR 2.5.1a (Suppl. Ref.3). Resultant expression tables were imported into Partek 6.6, (Partek Inc., St. Louis, MO, USA). Data was log2 transformed, quantile-normalized and analyzed using one-way ANOVA. *p*-values were corrected for multiple testing and genes with *q*-values < 0.05 and fold change >|2| were selected for further analysis.

Immunoblotting

Liver tissues were lysed in RIPA Lysis Buffer System (Santa Cruz Technology, Dallas, TX, USA) for 1 h at 4°C with gentle shaking. The cell lysate was centrifuged at 15,000*g* for 20 min at 4°C to eliminate cell debris. Total protein concentration was determined by the Bradford Protein Assay (Bio-Rad, Hercules, CA, USA). 50 µg of total protein per sample were separated on 12% gels and then electroblotted onto PVDF membranes (GE Healthcare Life Sciences, Pittsburgh, PA, USA). Membranes were probed overnight with anti-α-SMA (Abcam, Cambridge, MA, USA) (#ab5694, 1:1,000), anti-TREM-1 (Abcam) (#ab106153, 1:1,000) and anti-β-actin (Sigma Aldrich) (#A3854, 1:40,000) antibodies. Secondary HRP-conjugated mouse (Cell Signaling Technology, Danvers, MA, USA) (#7076) or rabbit (Cell Signaling Technology) (#7074) antibodies were used at a dilution of 1:5,000. Membranes were developed using enhanced

chemiluminescence system (Thermo Fisher Scientific). Protein quantification was performed with the Image J software.

Depletion and adoptive transfer of Kupffer cells

For ablation of endogenous Kupffer cells, 200 µl of clodronate-containing liposome suspensions (from Dr. N. Van Rooijen, VUMC, Amsterdam, The Netherlands) were administered by *i.p*. injection to WT and *Trem1*$^{-/-}$ mice. Depletion of Kupffer cells was assessed at 72 h by immunofluorescence staining of live sections with FITC-conjugated rat anti-mouse F4/80 antibody (Biolegend) (#123108, clone BM8). Donor Kupffer cells were isolated from collagenase type I-perfused livers of WT mice as described above. 10^5 Kupffer cells were transferred by *i.v*. 72 h after injection of liposomes into each host mouse. Adoptively transferred cells were observed by immunofluorescence staining, as described above, 96 h after transplantation. Mice with adoptively transferred Kupffer cells were given one dose of CCl_4 (2 µl/g) at 72 h-post-injection of clodronate and sacrificed 72 h-post-CCl_4 injection.

Quantitative assessment of uptake and distribution of reticulo-endothelial system specific nanoparticles during liver fibrogenesis

8-week-old male WT mice or *Trem1*$^{-/-}$ mice were injected with oil (control) or CCl_4 (2 µl/g) twice per week over a 6-week period and then were injected with 30 µl of Mvivo BIS (MediLumine, Montreal, Canada) (#SKU BIS-200) 3 h before being transferred to a small-animal CT scanner (nanoScan® SC, Mediso, Budapest, Hungary). Anesthesia was induced by inhalation of 1.5%-2% isoflurane in 100% oxygen. The animals were placed in an imaging chamber especially designed for small-animal CT studies to allow for temperature control and monitoring, reproducible positioning and anesthesia delivery. Analysis of the CT scan data was performed with Image J and GraphPad Prism software.

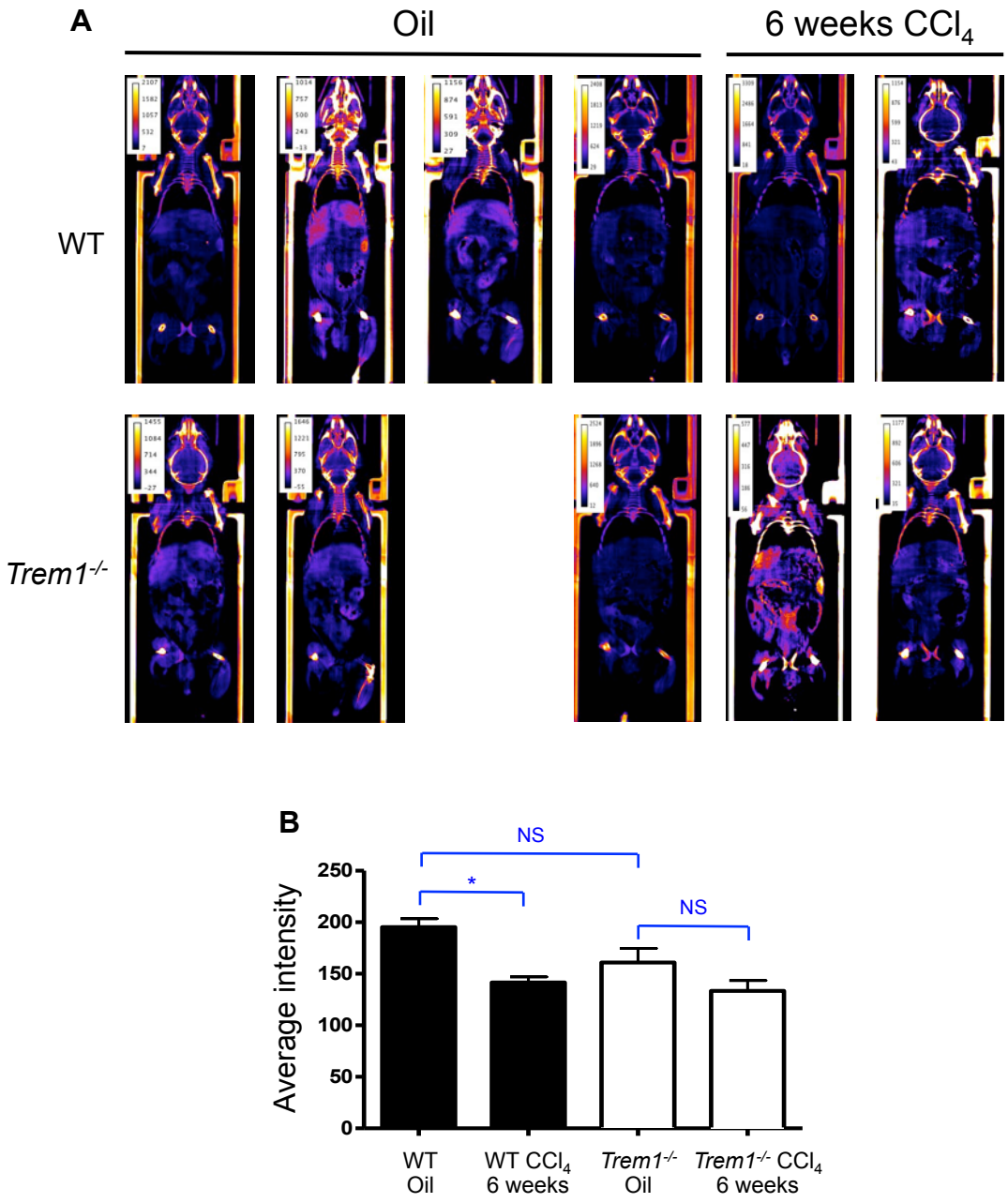

Figure S1. Deletion of *Trem1* attenuates hepatic reticuloendothelial function during liver fibrogenesis. WT and *Trem1*$^{-/-}$ mice were injected with CCl_4 for 6 weeks. The function of the hepatic reticuloendothelial system was determined by CT Scan with Mvivo BIS reagent. (**A**) Mice were injected with 30 µl of Mvivo BIS 3 h before undergoing CT imaging scan. Liver injury was measured by the efficiency of Mvivo BIS uptake by Kupffer cells. Coronal slices of CT scan from WT control (n = 3), *Trem1*$^{-/-}$ control (n = 2), WT and *Trem1*$^{-/-}$ CCl_4-injured mice (n = 3 per group) are shown. (**B**) The hepatic reticuloendothelial system function was determined by measuring the average intensity from 40 liver sections/mouse. Results are displayed as mean ± SEM. *$p < 0.05$. ANOVA followed by Bonferroni's post hoc test was used in **B.**

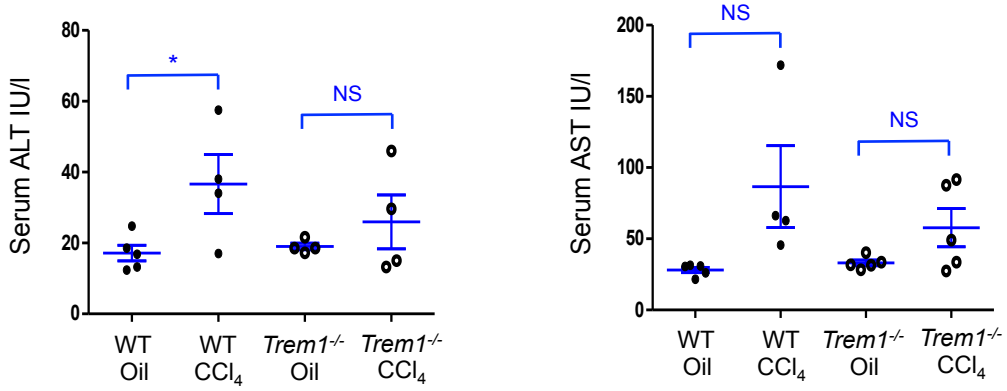

Figure S2. TREM-1 deficiency decreases sensitivity for development of liver injury. Serum ALT and AST levels from WT and *Trem1*$^{-/-}$ control mice (oil) or 6 weeks CCl_4-treated mice were measured with colorimetric assay (n = 4-5 per group). Results are displayed as mean ± SEM. *$p < 0.05$. Two-tailed Student's *t* test was used.

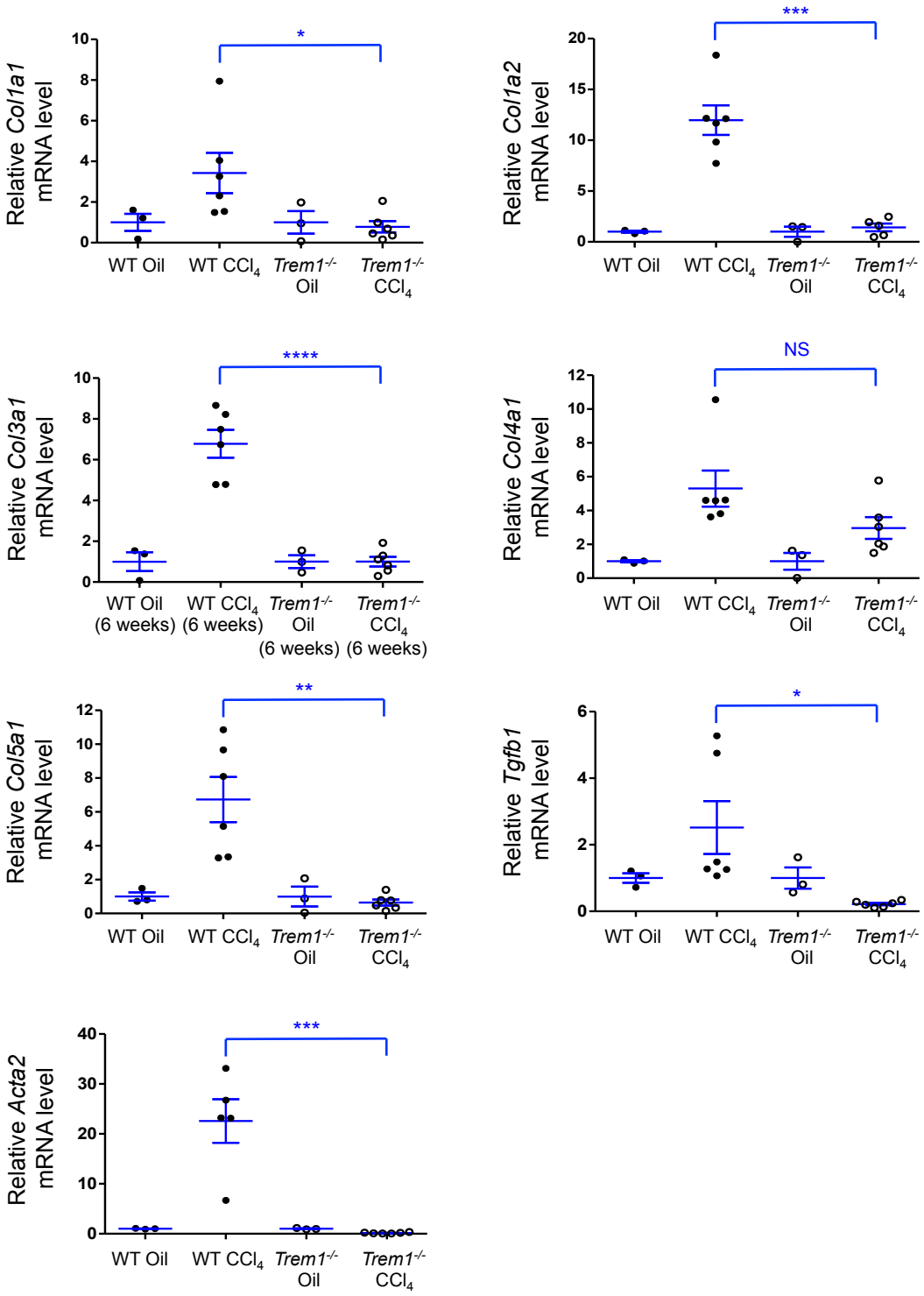

Figure S3. Deletion of *Trem1* reduces expression of genes involved in hepatic fibrogenesis. Hepatic levels of *Col1a1*, *Col1a2*, *Col3a1*, *Col4a1*, *Col5a1*, *Tgfb1* and *Acta2* mRNA were assessed by RT-qPCR for WT and *Trem1*$^{-/-}$ 6 weeks CCl_4-treated (n = 5-6 per group) and control (oil-treated, n = 3 per group) mice. The gene expression was normalized to *Actb, Hprt1* and *rRNA 18S* levels, and the expression of each gene relative to oil-treated WT and *Trem1*$^{-/-}$ mice is depicted. Results are displayed as mean ± SEM. *$p < 0.05$, **$p < 0.01$,*** $p < 0.001$, **** $p < 0.0001$. Two-tailed Student's *t* test was used.

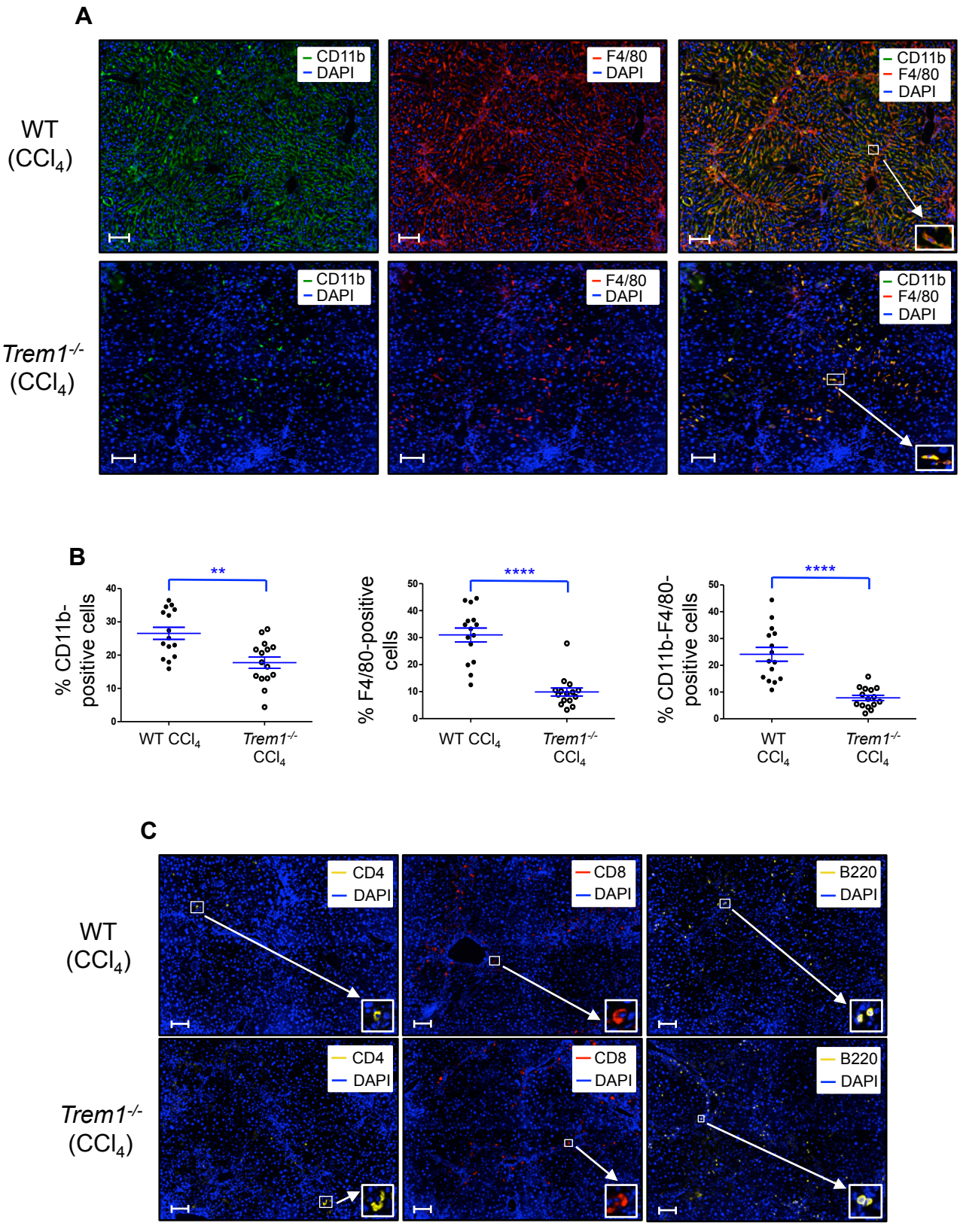
A
WT (CCl4)
Trem1-/- (CCl4)
CD11b
DAPI
F4/80
CD11b
F4/80
DAPI
B
% CD11b-positive cells
% F4/80-positive cells
% CD11b-F4/80-positive cells
**
****
****
WT CCl4
Trem1-/- CCl4
C
CD4
CD8
B220
DAPI

Figure S4. Deletion of *Trem1* reduces CD11b-, F4/80-, and CD11b-F4/80-positive cell infiltration. WT and *Trem1*$^{-/-}$ mice were treated with CCl_4 for 6 weeks. **(A)** Representative images of fluorescent-multiplexed immunohistochemistry of WT and *Trem1*$^{-/-}$ mouse liver samples. Samples were stained for CD11b (green), F4/80 (red) and DAPI (blue) (n = 3 mice per group, original magnification, x20; scale bar, 50 μm). (**B**) Quantification of CD11b, F4/80 and CD11b-F4/80-positive cells (n = 5 areas/mouse) from WT and *Trem1*$^{-/-}$ 6 week CCl_4-treated mice. (**C**) Representative images of fluorescent-multiplexed immunohistochemistry of WT and *Trem1*$^{-/-}$ mouse liver samples. Samples were stained for CD4 (yellow), CD8 (red), B220 (yellow) and DAPI (blue) (n = 3 mice per group, original magnification, x20; scale bar, 50 μm). Results are displayed as mean ± SEM. $^{**}p < 0.01$, $^{****}p < 0.0001$. Two-tailed Student's *t* test was used in **B.** Experiments shown in **A** and **C** are representative of 2 independent experiments

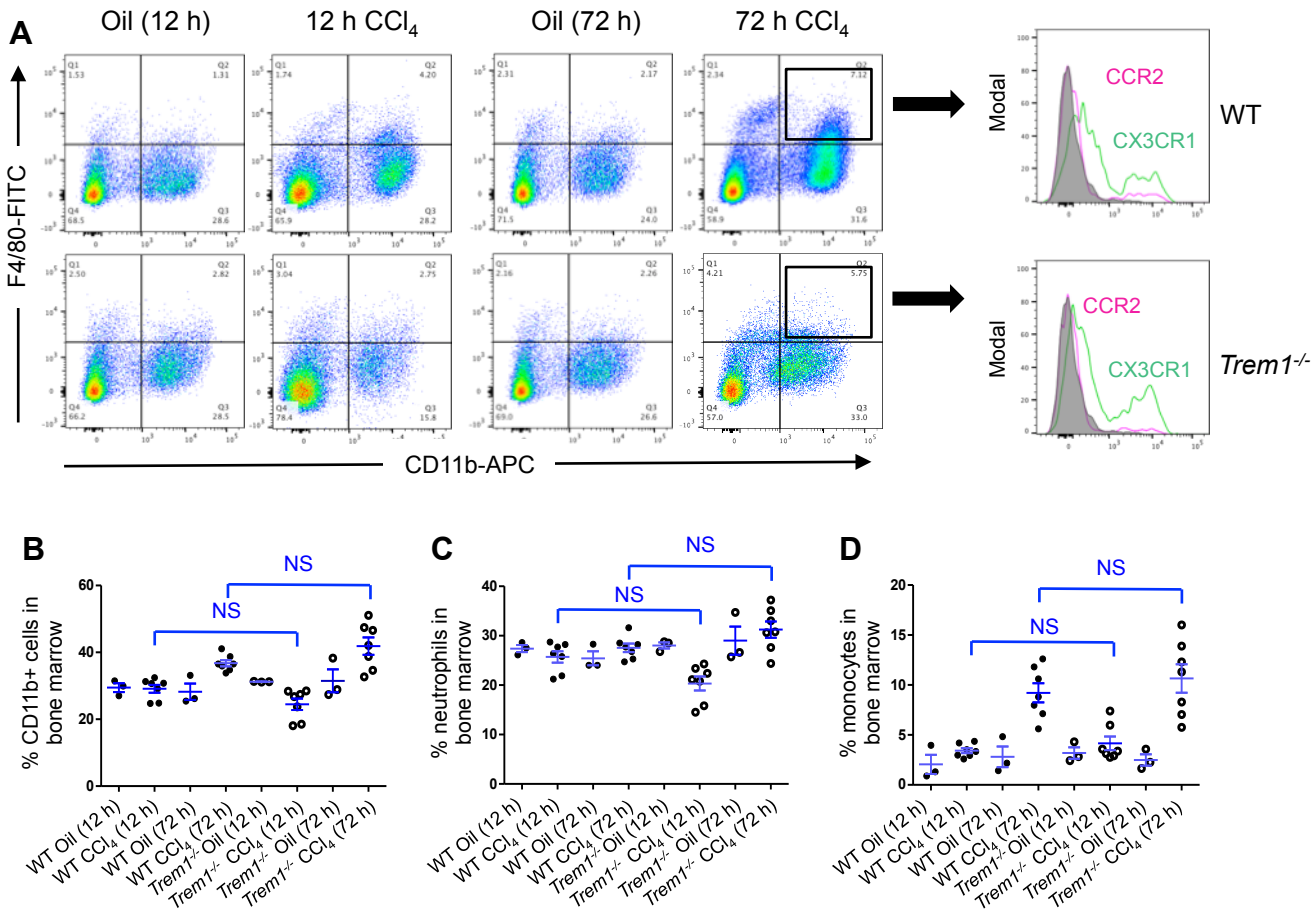
A
Oil (12 h)
12 h CCl4
Oil (72 h)
72 h CCl4
F4/80-FITC
CD11b-APC
Modal
CCR2
CX3CR1
WT
Trem1-/-
B
% CD11b+ cells in bone marrow
C
% neutrophils in bone marrow
D
% monocytes in bone marrow
NS
WT Oil (12 h)
WT CCl4 (12 h)
WT Oil (72 h)
WT CCl4 (72 h)
Trem1-/- Oil (12 h)
Trem1-/- CCl4 (12 h)
Trem1-/- Oil (72 h)
Trem1-/- CCl4 (72 h)
E
Oil (12 h)
12 h CCl4
Oil (72 h)
72 h CCl4
F4/80-FITC
CD11b-APC
Modal
CCR2
CX3CR1
WT
Trem1-/-
F
% CD11b+ cells in blood
G
% neutrophils in blood
H
% patrolling monocytes in blood
NS
***
**
WT Oil (12 h)
WT CCl4 (12 h)
WT Oil (72 h)
WT CCl4 (72 h)
Trem1-/- Oil (12 h)
Trem1-/- CCl4 (12 h)
Trem1-/- Oil (72 h)
Trem1-/- CCl4 (72 h)

Figure S5. Deletion of *Trem1* reduces inflammatory cell infiltration at early stages of liver fibrogenesis. WT and *Trem1*$^{-/-}$ mice were analyzed 6 h, 12 h, and 72 h after injection of single dose of CCl_4. Flow cytometry dot plots of bone marrow cells (**A-D**) and blood (**E-H**) cells from control WT and *Trem1*$^{-/-}$ (oil-injected, n = 3 per group), and WT and *Trem1*$^{-/-}$ mice (n = 7 mice/time-point/group) 12 h and 72 h after CCl_4 injury stained with anti-F4/80, anti-CD11b, anti-CCR2 and anti-CX3CR1 antibodies. Flow cytometry histograms of bone marrow (**A**) and blood (**E**) cells, gated on F4/80$^+$-CD11b$^+$, analyzed for the expression of CCR2 and CX3CR1 72 h after CCl_4 injection (n = 7 mice per group). Control staining was performed with IgG isotype (grey histograms). Percentage of CD11b$^+$ cells, neutrophils, and monocytes in bone marrow (**B-D**) and blood (**F-H**) from WT and *Trem1*$^{-/-}$ mice, quantified after 12 h and 72 h oil or CCl_4 treatment. Results are displayed as mean ± SEM. ** *p<0.01,* *** *p<0.001*. Two-tailed Student's *t* test was used in **B**, **C**, **D**, **F**, **G** and **H.**

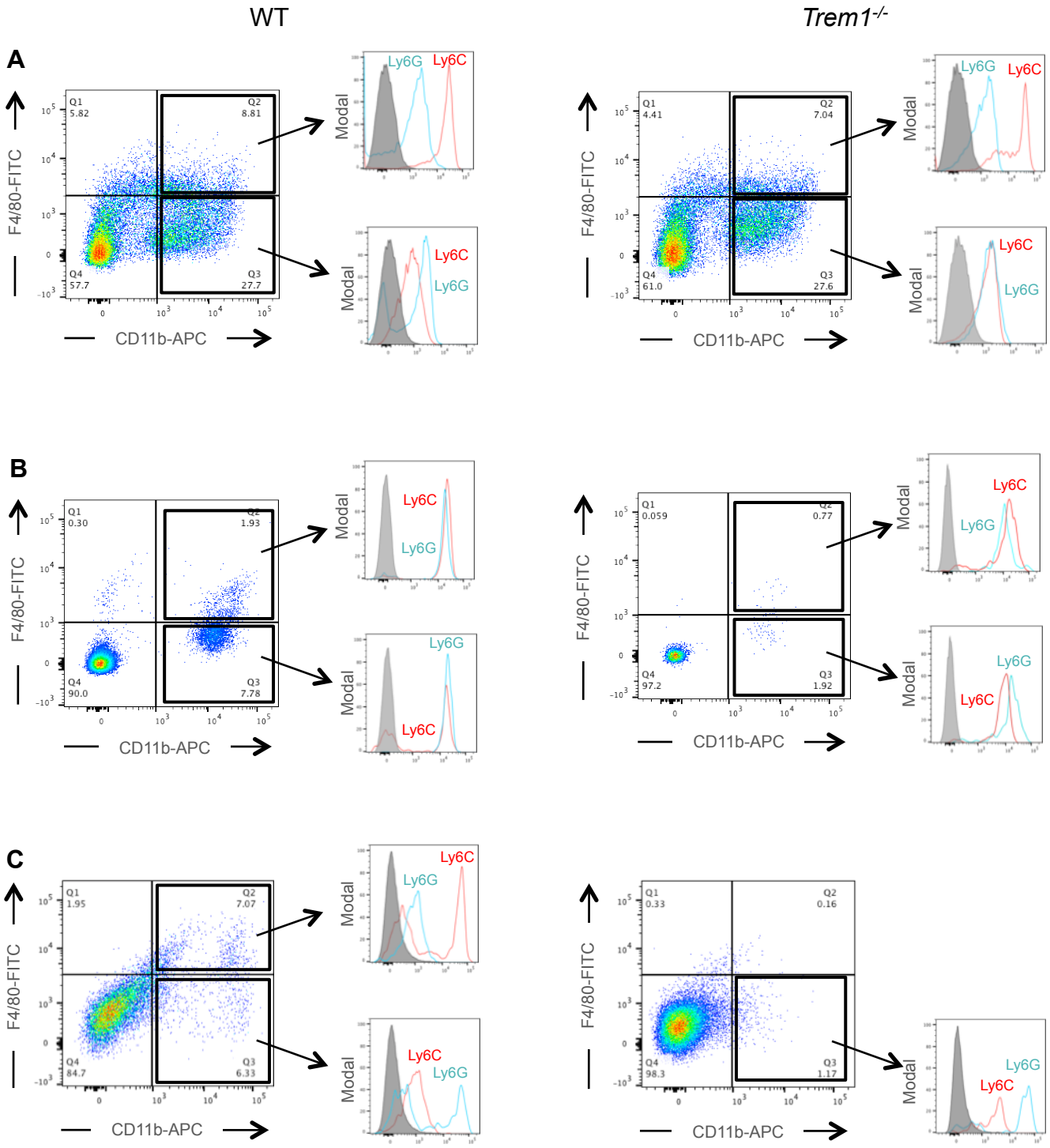

Figure S6. Characteristics of inflammatory cells recruited 72 h after CCl_4 treatment from bone marrow to peripheral blood and liver. Flow cytometry dot plots and histograms of bone marrow (**A**), blood (**B**) and liver (**C**) cells from WT and *Trem1*$^{-/-}$ mice (n = 7 per group) 72 h after CCl_4 injury stained with anti-F4/80, anti-CD11b, anti-Ly6C and anti-Ly6G antibodies. Control staining was performed with IgG isotype (grey histograms) .

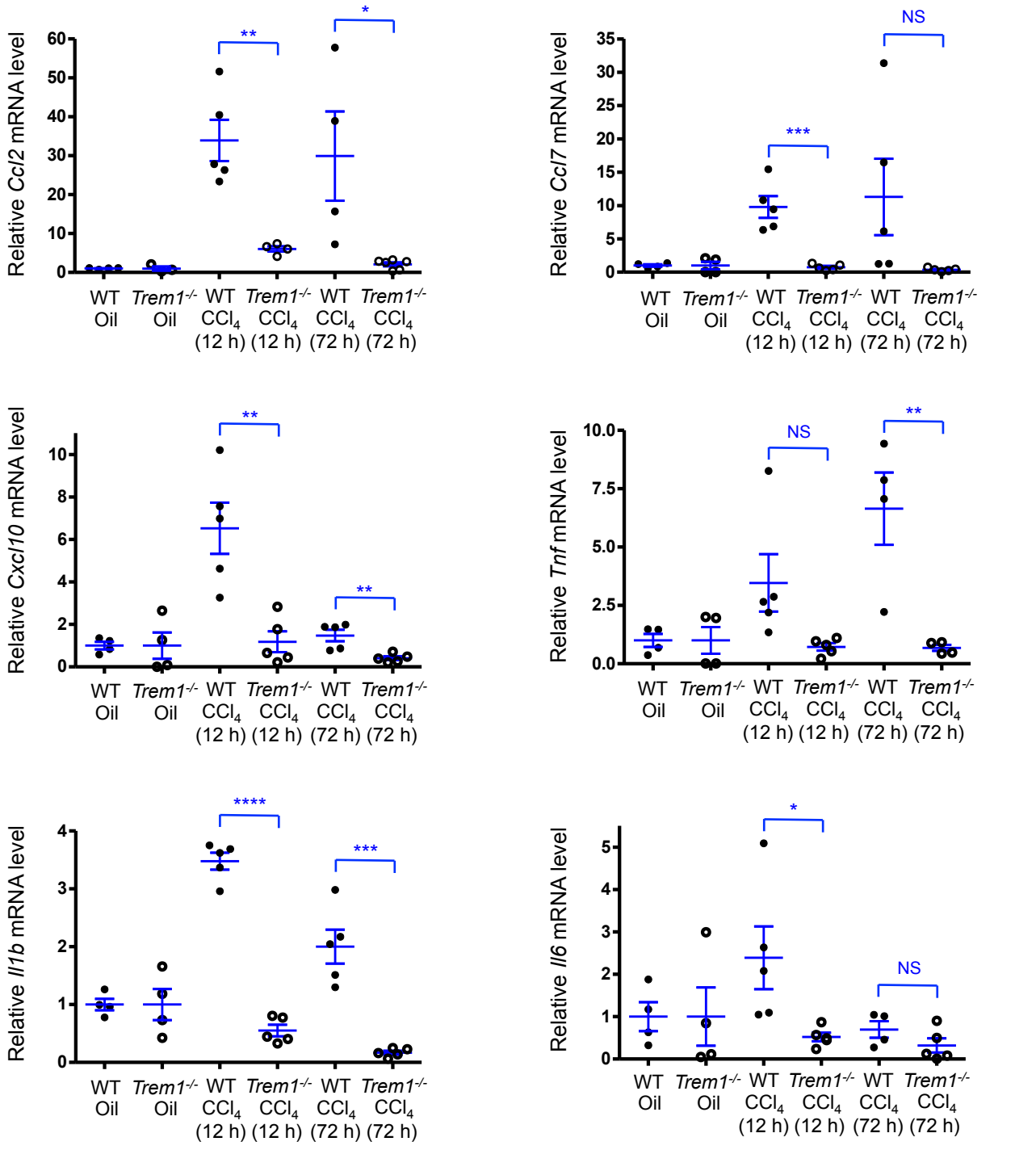

Figure S7. Deletion of *Trem1* reduces the expression of chemokines and cytokines during liver fibrogenesis. Mice were treated with oil or a single dose of CCl_4. Total RNA was isolated 12 h and 72 h after CCl_4 injection from livers of WT or *Trem1*$^{-/-}$ mice (n = 4-5 mice/time-point/group). *Ccl2, Ccl7, Cxcl10, Tnf, Il1b* and *Il6* mRNA levels were assessed by RT-qPCR and represented as fold-induction. The gene expression was normalized to *Actb, Hprt1* and *rRNA 18S* levels, and the expression of each gene relative to oil-treated WT and *Trem1*$^{-/-}$ mice (n = 3 mice/time-point/group) is depicted. Results are displayed as mean ± SEM. * *p<0.05, ** p<0.01, *** p<0.001*, **** *p<0.0001*. Two-tailed Student's *t* test was used.

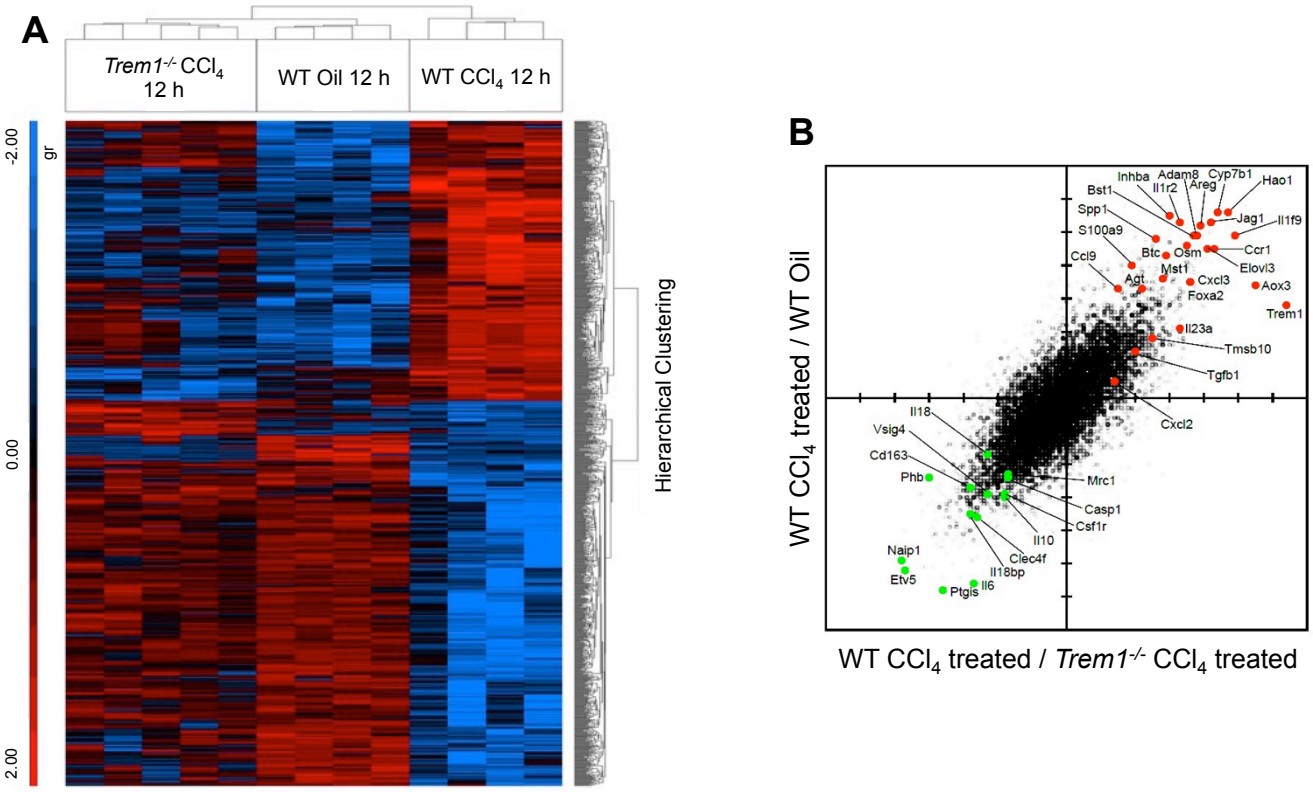

Figure S8. Deletion of *Trem1* on Kupffer cells reduces the expression of genes involved in fibrogenesis, metabolism and recruitment of inflammatory cells. RNA was extracted from Kupffer cells isolated from cohorts of 4 WT or 5 *Trem1*$^{-/-}$ mice per group 12 h post single dose of CCl_4 and from Kupffer cells isolated from cohorts of 4 oil-treated WT mice per group. Samples were processed using the Illumina NextSeq 500 and analyzed using the NIH Biowulf cluster, STAR 2.5.1a and Partek 6.6.The data shown in **A** were obtained from one RNAseq experiment run with 4 or 5 individual RNA samples per group. The heat map shows differentially expressed genes (≥ 2-fold change in expression (q-value < 0.05)). (**B**) Scatterplot shows on X axis the log2 ratios of the transcripts identified in Kupffer cells of WT CCl_4-treated mice *versus* transcripts of Kupffer cells from *Trem1*$^{-/-}$ CCl_4-treated mice and Y-axis shows log2 ratios of transcripts in WT CCl_4-treated and WT oil-treated mice. Genes of interest were chosen with a q-value threshold of < 0.05 and with fold change of > |2|.

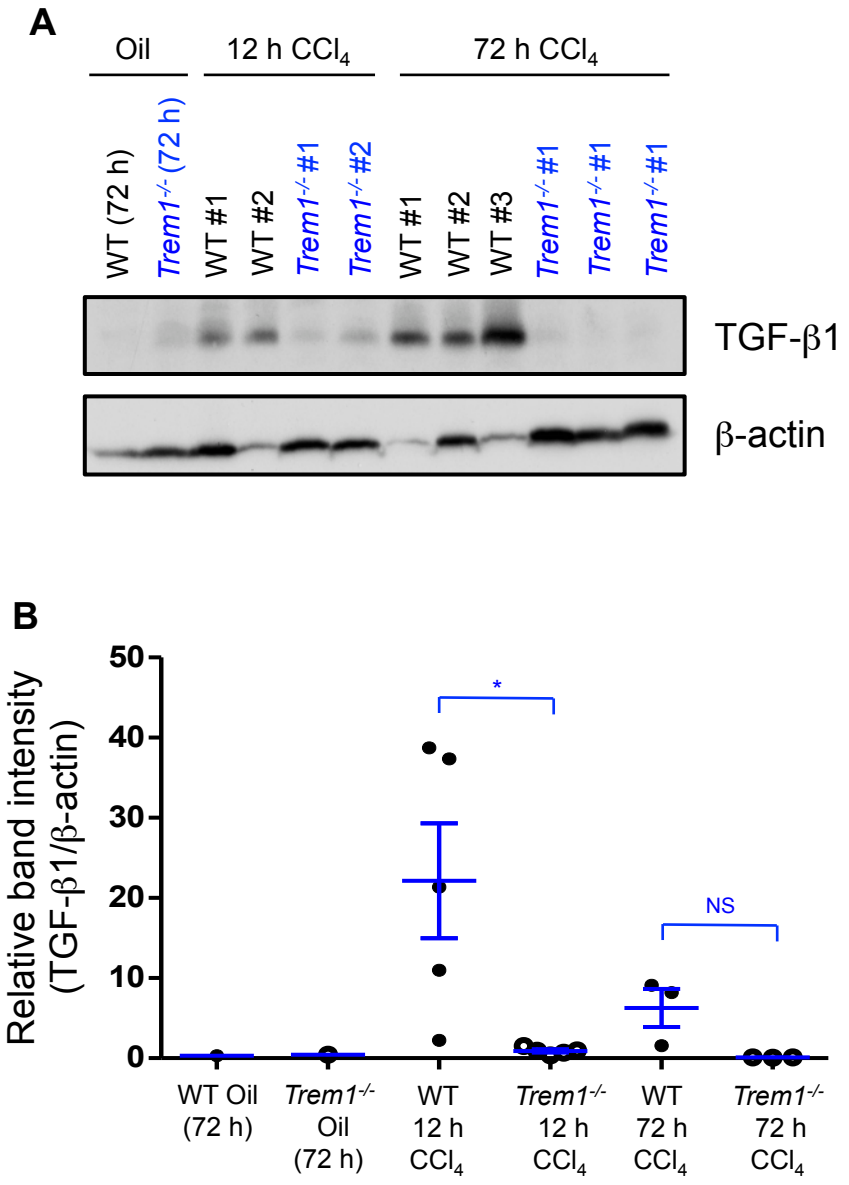

Figure S9. Deletion of *Trem1* reduces expression of TGF-β1. (**A**) Immunoblot analysis for TGF-β1 in liver lysates from indicated mice (n = 2 per group at 12 h after CCl_4 injury, n = 3 per group at 72 h after CCl_4 injury). β-actin was used as loading control. (**G**) Quantification of TGF-β1 expression (n = 5 mice per group at 12 h after CCl_4 injury, and n = 3 mice per group at 72 h after CCl_4 injury). Results are displayed as mean ± SEM. *$p < 0.05$. Two-tailed Student's *t* test was used in **B.**

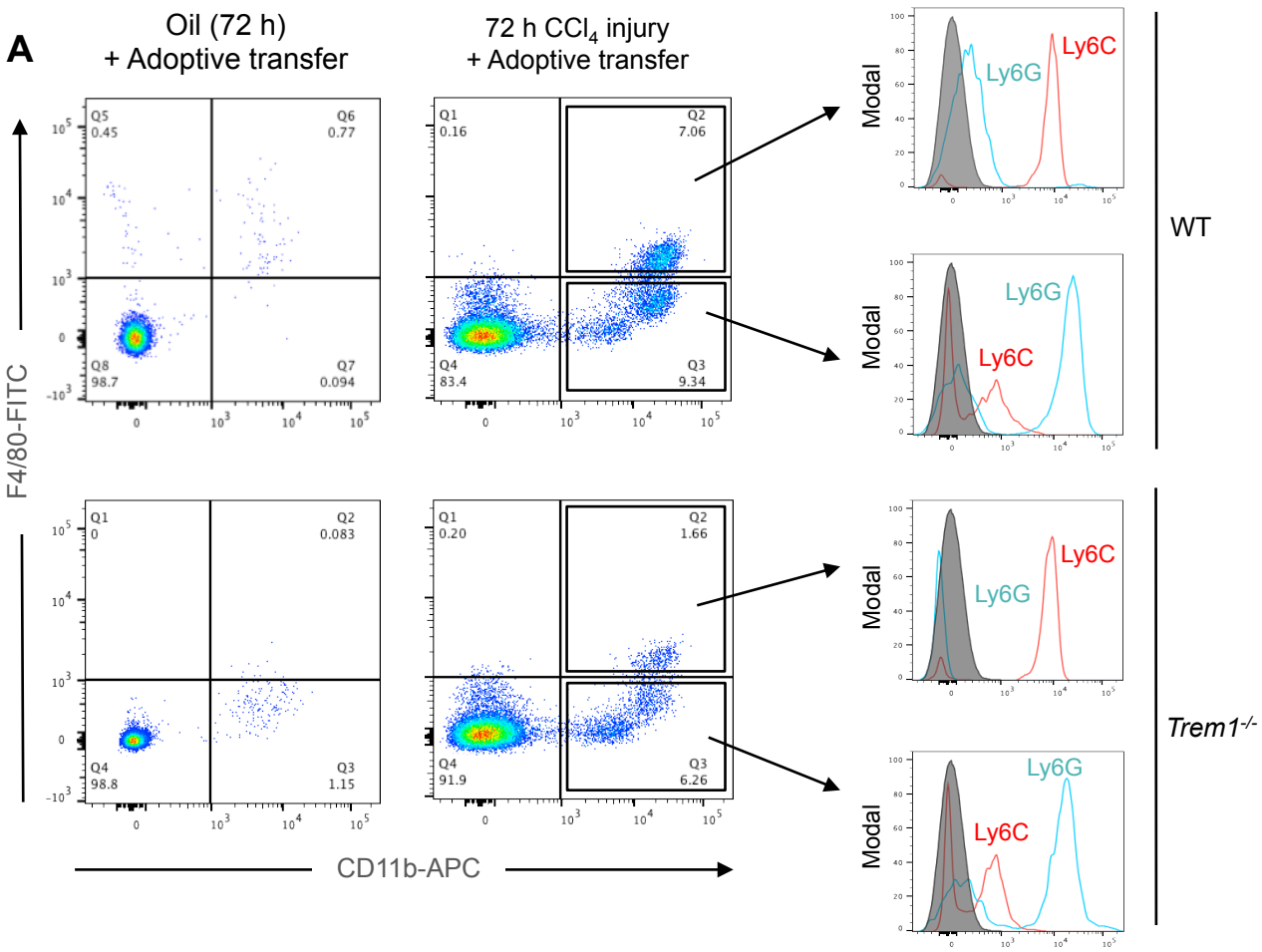
A
Oil (72 h)
+ Adoptive transfer
72 h CCl4 injury
+ Adoptive transfer
F4/80-FITC
CD11b-APC
Q5 0.45
Q6 0.77
Q8 98.7
Q7 0.094
Q1 0.16
Q2 7.06
Q4 83.4
Q3 9.34
Q1 0
Q2 0.083
Q4 98.8
Q3 1.15
Q1 0.20
Q2 1.66
Q4 91.9
Q3 6.26
Modal
Ly6G
Ly6C
WT
Trem1-/-

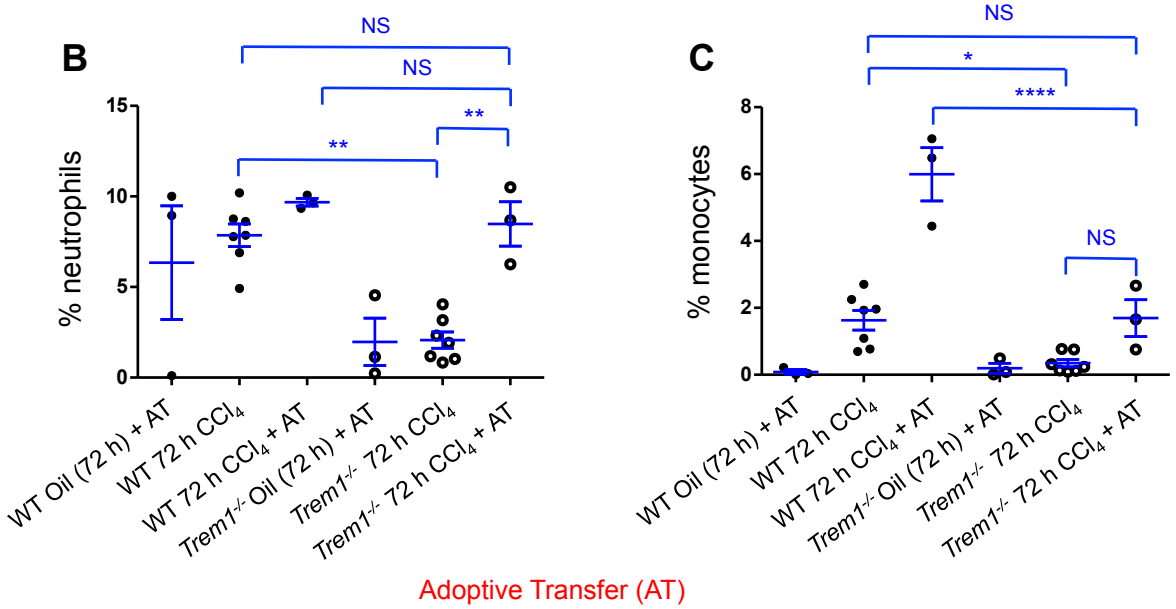
B
% neutrophils
NS
NS
**
**
C
% monocytes
NS
*
****
NS
WT Oil (72 h) + AT
WT 72 h CCl4
WT 72 h CCl4 + AT
Trem1-/- Oil (72 h) + AT
Trem1-/- 72 h CCl4
Trem1-/- 72 h CCl4 + AT
Adoptive Transfer (AT)

Figure S10. Adoptive transfer (AT) of Kupffer cells from WT mice increases recruitment of inflammatory cells to peripheral blood of *Trem1*$^{-/-}$ mice. **(A)** WT Kupffer cells were adoptively transferred into recipient of macrophage-depleted WT and *Trem1*$^{-/-}$ mice subsequently treated with CCl_4. Flow cytometry dot plots and histograms of peripheral blood mononuclear cells from WT and *Trem1*$^{-/-}$ control (adoptive transfer and oil-injected, n = 3 per group) and WT and *Trem1*$^{-/-}$ CCl_4-injected mice (adoptive transfer and CCl_4-injected, n = 3 per group) were stained with anti-F4/80, anti-CD11b, anti-Ly6C and anti-Ly6G antibodies. Control staining was performed with IgG isotype (grey histograms). Percentage of neutrophils (**B**) and patrolling monocytes (**C**) in WT and *Trem1*$^{-/-}$ mice (n = 3-7 per group). Results are displayed as mean ± SEM. * *p<0.05,* ** *p<0.01,* **** *p<0.0001*. ANOVA followed by Bonferroni's post hoc test was used in **B** and **C**.

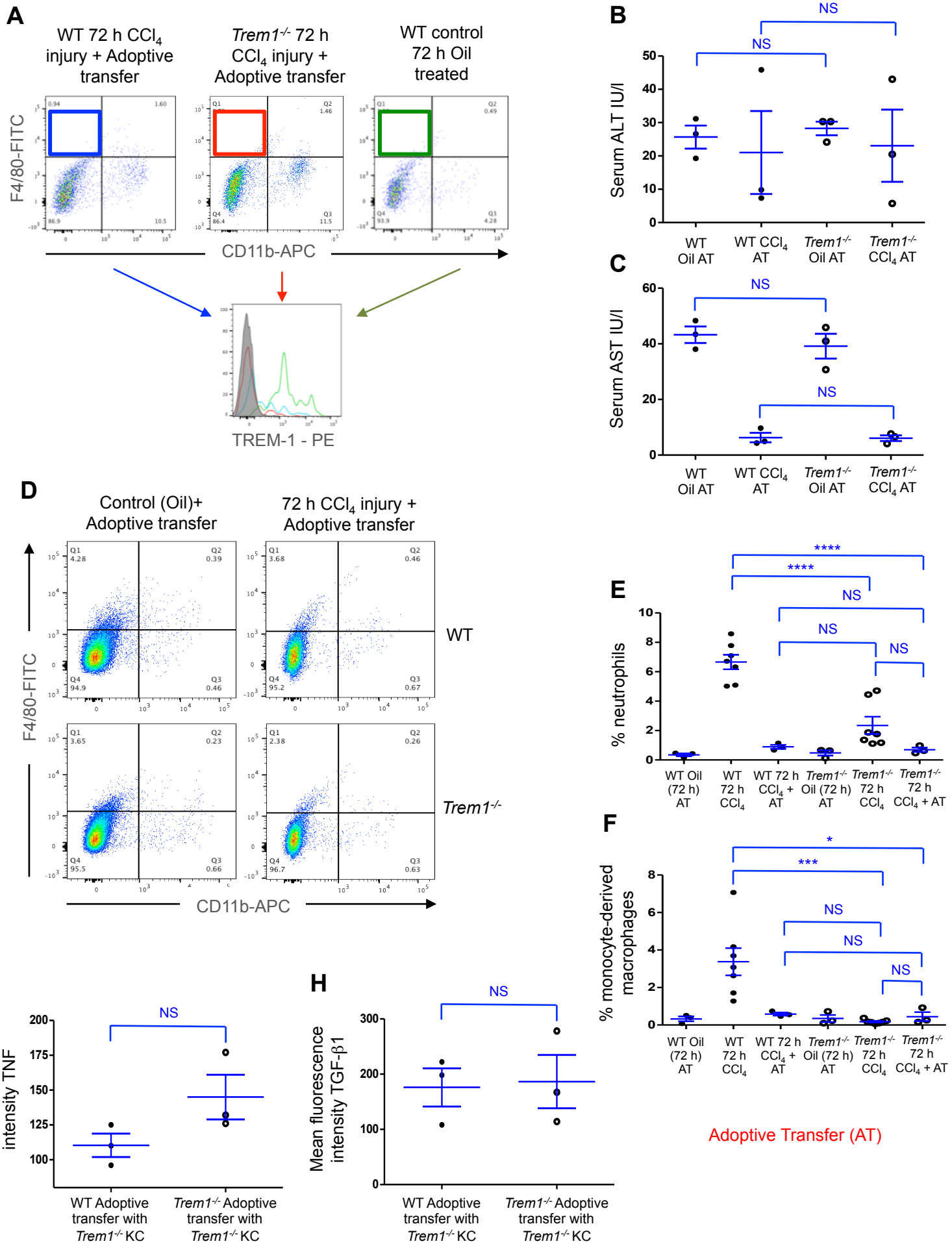
A
WT 72 h CCl4 injury + Adoptive transfer
Trem1-/- 72 h CCl4 injury + Adoptive transfer
WT control 72 h Oil treated
F4/80-FITC
CD11b-APC
TREM-1 - PE
B
Serum ALT IU/l
NS
WT Oil AT
WT CCl4 AT
Trem1-/- Oil AT
Trem1-/- CCl4 AT
C
Serum AST IU/l
NS
D
Control (Oil)+ Adoptive transfer
72 h CCl4 injury + Adoptive transfer
WT
Trem1-/-
F4/80-FITC
CD11b-APC
E
% neutrophils
****
NS
WT Oil (72 h) AT
WT 72 h CCl4
WT 72 h CCl4 + AT
Trem1-/- Oil (72 h) AT
Trem1-/- 72 h CCl4
Trem1-/- 72 h CCl4 + AT
F
% monocyte-derived macrophages
*
***
NS
Adoptive Transfer (AT)
G
Mean fluorescence intensity TNF
NS
WT Adoptive transfer with Trem1-/- KC
Trem1-/- Adoptive transfer with Trem1-/- KC
H
Mean fluorescence intensity TGF-β1
NS

Figure S11. Adoptive transfer (AT) of Kupffer cells from *Trem1*$^{-/-}$ mice reduces liver injury and recruitment of inflammatory cells in WT mice. (**A**) Flow cytometry dot plots and histogram of TREM-1 expression on Kupffer cells, after adoptive transfer of *Trem1*$^{-/-}$ Kupffer cells to WT and *Trem1*$^{-/-}$ mice and WT control oil-treated mice without adoptive transfer (n = 3 per group). Control staining was performed with IgG isotype (grey histograms). (**B**) Serum ALT and (**C**) AST levels from WT and *Trem1*$^{-/-}$ mice with adoptive transfer of *Trem1*-deficient Kupffer cells followed by single dose of CCl_4 treatment were measured at 72 h post CCl_4 injury with colorimetric assay (n = 3 mice per group). (**D-H**) Macrophage-depleted WT and *Trem1*$^{-/-}$ mice were adoptively transferred with *Trem1*-deficient Kupffer cells following treatment with a single dose of CCl_4. Flow cytometry dot plots of liver cells stained with anti-F4/80, anti-CD11b, anti-TNF, anti-TGF-β1 antibodies and analyzed (n = 3 mice per group). (**E** and **F**) Percentage of liver-infiltrated neutrophils and inflammatory monocytes/monocyte-derived macrophages in indicated experimental conditions in WT and *Trem1*$^{-/-}$ mice (n = 3-7 per group). Mean fluorescence intensity of TNF (**G**) and TGF-β1 (**H**) shown on gated F4/80^{+}-CD11b^{-} (Kupffer cells) (n = 3 mice per group). Results are displayed as mean ± SEM. ** p<0.05, *** p<0.001, **** p<0.0001*. Two-tailed Student's *t* test was used in **B**, **C**, **G** and **H**. ANOVA followed by Bonferroni's post hoc test was used in **E** and **F**

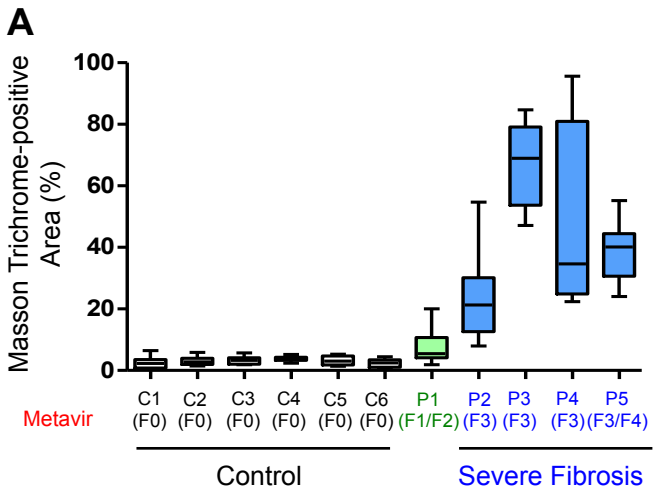

B

	C1 (F0)	C2 (F0)	C3 (F0)	C4 (F0)	C5 (F0)	C6 (F0)	P1 (F1/F2)	P2 (F3)	P3 (F3)	P4 (F3)	P5 (F3/F4)
C1 (F0)		0.8621	0.8106	0.6919	0.8223	0.9965	0.1954	<.0001	<.0001	<.0001	<.0001
C2 (F0)	0.8621		0.9321	0.8072	0.9481	0.8504	0.2202	<.0001	<.0001	<.0001	<.0001
C3 (F0)	0.8106	0.9321		0.8906	0.9834	0.7963	0.2904	<.0001	<.0001	<.0001	<.0001
C4 (F0)	0.6919	0.8072	0.8906		0.8699	0.6623	0.3149	<.0001	<.0001	<.0001	<.0001
C5 (F0)	0.8223	0.9481	0.9834	0.8699		0.8083	0.2702	<.0001	<.0001	<.0001	<.0001
C6 (F0)	0.9965	0.8504	0.7963	0.6623	0.8083		0.1577	<.0001	<.0001	<.0001	<.0001
P1 (F1/F2)	0.1954	0.2202	0.2904	0.3149	0.2702	0.1577		<.0001	<.0001	<.0001	<.0001
P2 (F3)	<.0001	<.0001	<.0001	<.0001	<.0001	<.0001	<.0001		<.0001	<.0001	<.0001
P3 (F3)	<.0001	<.0001	<.0001	<.0001	<.0001	<.0001	<.0001	<.0001		0.0001	<.0001
P4 (F3)	<.0001	<.0001	<.0001	<.0001	<.0001	<.0001	<.0001	<.0001	0.0001		0.0992
P5 (F3/F4)	<.0001	<.0001	<.0001	<.0001	<.0001	<.0001	<.0001	<.0001	<.0001	0.0992	

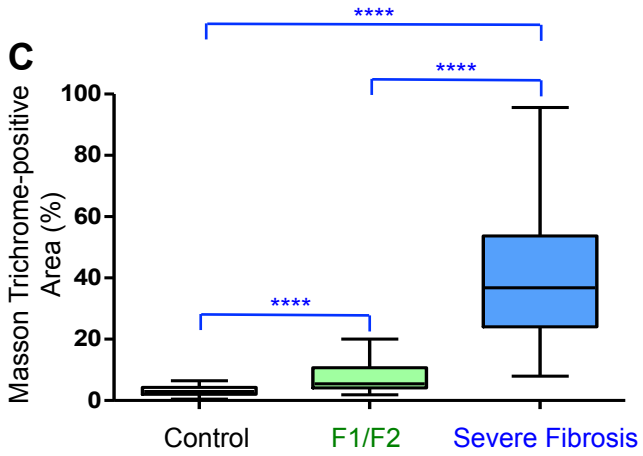

Figure S12. Collagen deposition increases in patients with liver fibrosis. Human liver samples from 6 controls (C1 to C6, Stage F0), a patient diagnosed with stage F1/F2 (P1) and 4 patients (P2 to P5) diagnosed with severe liver fibrosis (≥ F3) were stained with Masson Trichrome for collagen deposition. **(A)** Quantification of Masson Trichrome-positive area (%) from each sample (of at least 4 areas per sample). Boxplots with whiskers indicate the Least Square Mean (LSM), including maximum and minimum values and the median value of the data set. **(B)** LSM test was used to analyze the mean difference between any pair of subjects without multiplicity adjustments. Table represents *p*-values between any pair of subjects. A *p*-value less than 0.05 was considered to be statistically significant. **(C)** One-way ANOVA was used to test the mean between control group, F1/F2 patient and severe fibrosis group. Pair-wise comparisons indicated a *p*-value <0.0001 between any pair of groups.

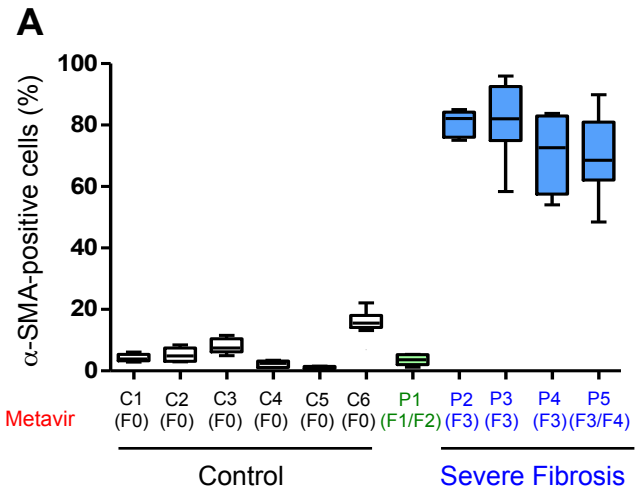

B

	C1 (F0)	C2 (F0)	C3 (F0)	C4 (F0)	C5 (F0)	C6 (F0)	P1 (F1/F2)	P2 (F3)	P3 (F3)	P4 (F3)	P5 (F3/F4)
C1 (F0)		0.8489	0.4293	0.6845	0.5369	0.0108	0.9088	<.0001	<.0001	<.0001	<.0001
C2 (F0)	0.8489		0.548	0.551	0.4197	0.0192	0.7603	<.0001	<.0001	<.0001	<.0001
C3 (F0)	0.4293	0.548		0.2331	0.1614	0.0934	0.366	<.0001	<.0001	<.0001	<.0001
C4 (F0)	0.6845	0.551	0.2331		0.8323	0.0029	0.7704	<.0001	<.0001	<.0001	<.0001
C5 (F0)	0.5369	0.4197	0.1614	0.8323		0.0014	0.6148	<.0001	<.0001	<.0001	<.0001
C6 (F0)	0.0108	0.0192	0.0934	0.0029	0.0014		0.0075	<.0001	<.0001	<.0001	<.0001
P1 (F1/F2)	0.9088	0.7603	0.366	0.7704	0.6148	0.0075		<.0001	<.0001	<.0001	<.0001
P2 (F3)	<.0001	<.0001	<.0001	<.0001	<.0001	<.0001	<.0001		0.6213	0.0214	0.0052
P3 (F3)	<.0001	<.0001	<.0001	<.0001	<.0001	<.0001	<.0001	0.6213		0.0026	0.0001
P4 (F3)	<.0001	<.0001	<.0001	<.0001	<.0001	<.0001	<.0001	0.0214	0.0026		0.9837
P5 (F3/F4)	<.0001	<.0001	<.0001	<.0001	<.0001	<.0001	<.0001	0.0052	0.0001	0.9837	

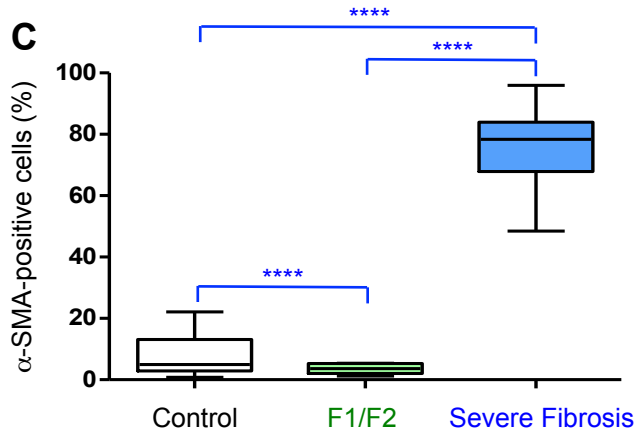

Figure S13. The number of α-SMA-positive cells increases in patients with severe fibrosis. Human liver samples from 6 controls (C1 to C6, Stage F0), a patient diagnosed with stage F1/F2 (P1) and 4 patients (P2 to P5) diagnosed with severe liver fibrosis (≥ F3) were stained with anti-α-SMA antibody. **(A)** Quantification of α-SMA-positive cells (%) from each sample (of at least 5 areas per sample). Boxplots with whiskers indicate the Least Square Mean (LSM), including maximum and minimum values and the median value of the data set. **(B)** LSM test was used to analyze the mean difference between any pair of subjects without multiplicity adjustments. Table represents *p*-values between any pair of subjects. A *p*-value less than 0.05 was considered to be statistically significant. **(C)** One-way ANOVA was used to test the mean between control group, F1/F2 patient and severe fibrosis group. Pair-wise comparisons indicated a *p*-value <0.0001 between any pair of groups.

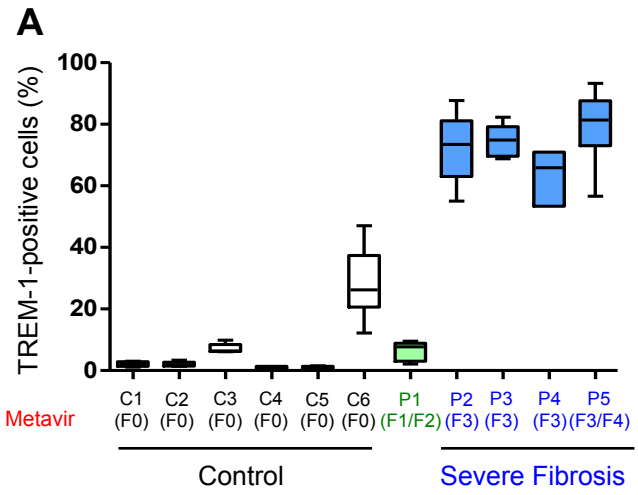

B

	C1 (F0)	C2 (F0)	C3 (F0)	C4 (F0)	C5 (F0)	C6 (F0)	P1 (F1/F2)	P2 (F3)	P3 (F3)	P4 (F3)	P5 (F3/F4)
C1 (F0)		0.9913	0.2971	0.813	0.8319	<.0001	0.3839	<.0001	<.0001	<.0001	<.0001
C2 (F0)	0.9913		0.2921	0.8215	0.8404	<.0001	0.3781	<.0001	<.0001	<.0001	<.0001
C3 (F0)	0.2971	0.2921		0.2023	0.2108	<.0001	0.8617	<.0001	<.0001	<.0001	<.0001
C4 (F0)	0.813	0.8215	0.2023		0.9807	<.0001	0.2695	<.0001	<.0001	<.0001	<.0001
C5 (F0)	0.8319	0.8404	0.2108	0.9807		<.0001	0.28	<.0001	<.0001	<.0001	<.0001
C6 (F0)	<.0001	<.0001	<.0001	<.0001	<.0001		<.0001	<.0001	<.0001	<.0001	<.0001
P1 (F1/F2)	0.3839	0.3781	0.8617	0.2695	0.28	<.0001		<.0001	<.0001	<.0001	<.0001
P2 (F3)	<.0001	<.0001	<.0001	<.0001	<.0001	<.0001	<.0001		0.661	0.1093	0.033
P3 (F3)	<.0001	<.0001	<.0001	<.0001	<.0001	<.0001	<.0001	0.661		0.0494	0.1051
P4 (F3)	<.0001	<.0001	<.0001	<.0001	<.0001	<.0001	<.0001	0.1093	0.0494		0.0006
P5 (F3/F4)	<.0001	<.0001	<.0001	<.0001	<.0001	<.0001	<.0001	0.033	0.1051	0.0006	

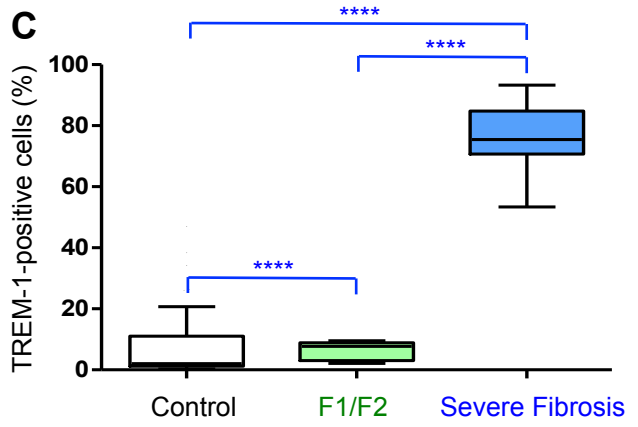

Figure S14. The number of TREM-1-positive cells increases in patients with severe fibrosis. Human liver samples from 6 controls (C1 to C6, Stage F0), a patient diagnosed with stage F1/F2 (P1) and 4 patients (P2 to P5) diagnosed with severe liver fibrosis (≥ F3) were stained with anti-TREM-1 antibody. **(A)** Quantification of TREM-1-positive cells (%) from each sample (of at least 5 areas per sample). Boxplots with whiskers indicate the Least Square Mean (LSM), including maximum and minimum values and the median value of the data set. **(B)** LSM test was used to analyze the mean difference between any pair of subjects without multiplicity adjustments. Table represents *p*-values between any pair of subjects. A *p*-value less than 0.05 was considered to be statistically significant. **(C)** One-way ANOVA was used to test the mean between control group, F1/F2 patient and severe fibrosis group. Pair-wise comparisons indicated a *p*-value <0.0001 between any pair of groups.

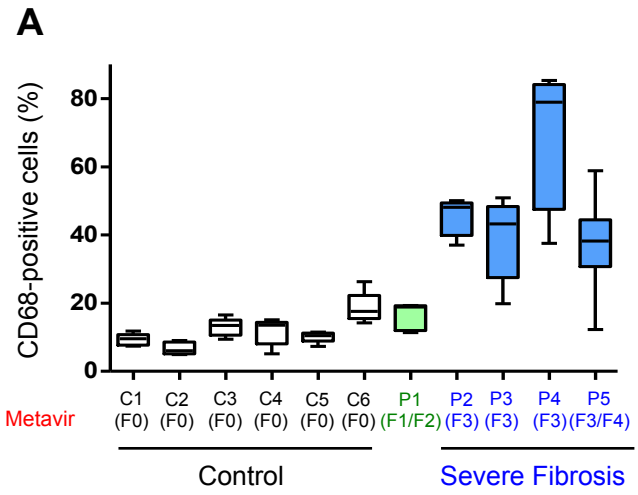

B

	C1 (F0)	C2 (F0)	C3 (F0)	C4 (F0)	C5 (F0)	C6 (F0)	P1 (F1/F2)	P2 (F3)	P3 (F3)	P4 (F3)	P5 (F3/F4)
C1 (F0)		0.6429	0.5134	0.6683	0.8811	0.064	0.2155	<.0001	<.0001	<.0001	<.0001
C2 (F0)	0.6429		0.2658	0.3736	0.5401	0.0194	0.0912	<.0001	<.0001	<.0001	<.0001
C3 (F0)	0.5134	0.2658		0.8212	0.6137	0.2509	0.5542	<.0001	<.0001	<.0001	<.0001
C4 (F0)	0.6683	0.3736	0.8212		0.78	0.1635	0.4145	<.0001	<.0001	<.0001	<.0001
C5 (F0)	0.8811	0.5401	0.6137	0.78		0.0904	0.2749	<.0001	<.0001	<.0001	<.0001
C6 (F0)	0.064	0.0194	0.2509	0.1635	0.0904		0.619	<.0001	0.0002	<.0001	<.0001
P1 (F1/F2)	0.2155	0.0912	0.5542	0.4145	0.2749	0.619		<.0001	0.0001	<.0001	<.0001
P2 (F3)	<.0001	<.0001	<.0001	<.0001	<.0001	<.0001	<.0001		0.2569	<.0001	0.0653
P3 (F3)	<.0001	<.0001	<.0001	<.0001	<.0001	0.0002	0.0001	0.2569		<.0001	0.626
P4 (F3)	<.0001	<.0001	<.0001	<.0001	<.0001	<.0001	<.0001	<.0001	<.0001		<.0001
P5 (F3/F4)	<.0001	<.0001	<.0001	<.0001	<.0001	<.0001	<.0001	0.0653	0.626	<.0001	

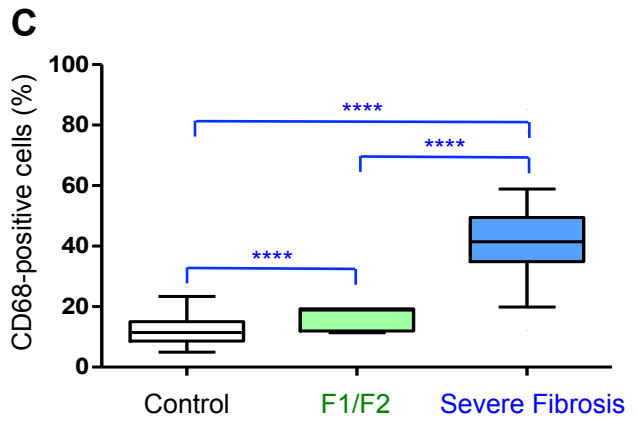

Figure S15. The number of CD68-positive cells increases in patients with severe fibrosis. Human liver samples from 6 controls (C1 to C6, Stage F0), a patient diagnosed with stage F1/F2 (P1) and 4 patients (P2 to P5) diagnosed with severe liver fibrosis (≥ F3) were stained with anti-CD68 antibody. **(A)** Quantification of CD68-positive cells (%) from each sample (of at least 5 areas per sample). Boxplots with whiskers indicate the Least Square Mean (LSM), including maximum and minimum values and the median value of the data set. **(B)** LSM test was used to analyze the mean difference between any pair of subjects without multiplicity adjustments. Table represents *p*-values between any pair of subjects. A *p*-value less than 0.05 was considered to be statistically significant. **(C)** One-way ANOVA was used to test the mean between control group, F1/F2 patient and severe fibrosis group. Pair-wise comparisons indicated a *p*-value <0.0001 between any pair of groups.

A

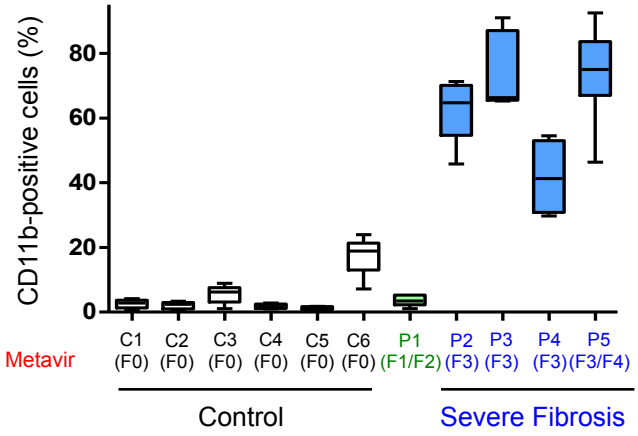

B

	C1 (F0)	C2 (F0)	C3 (F0)	C4 (F0)	C5 (F0)	C6 (F0)	P1 (F1/F2)	P2 (F3)	P3 (F3)	P4 (F3)	P5 (F3/F4)
C1 (F0)		0.9221	0.5587	0.8825	0.799	0.0019	0.8272	<.0001	<.0001	<.0001	<.0001
C2 (F0)	0.9221		0.4953	0.96	0.8753	0.0013	0.7521	<.0001	<.0001	<.0001	<.0001
C3 (F0)	0.5587	0.4953		0.4643	0.4022	0.0119	0.7136	<.0001	<.0001	<.0001	<.0001
C4 (F0)	0.8825	0.96	0.4643		0.9149	0.0011	0.7144	<.0001	<.0001	<.0001	<.0001
C5 (F0)	0.799	0.8753	0.4022	0.9149		0.0008	0.6366	<.0001	<.0001	<.0001	<.0001
C6 (F0)	0.0019	0.0013	0.0119	0.0011	0.0008		0.0038	<.0001	<.0001	<.0001	<.0001
P1 (F1/F2)	0.8272	0.7521	0.7136	0.7144	0.6366	0.0038		<.0001	<.0001	<.0001	<.0001
P2 (F3)	<.0001	<.0001	<.0001	<.0001	<.0001	<.0001	<.0001		0.0277	0.0002	0.0046
P3 (F3)	<.0001	<.0001	<.0001	<.0001	<.0001	<.0001	<.0001	0.0277		<.0001	0.8357
P4 (F3)	<.0001	<.0001	<.0001	<.0001	<.0001	<.0001	<.0001	0.0002	<.0001		<.0001
P5 (F3/F4)	<.0001	<.0001	<.0001	<.0001	<.0001	<.0001	<.0001	0.0046	0.8357	<.0001	

C

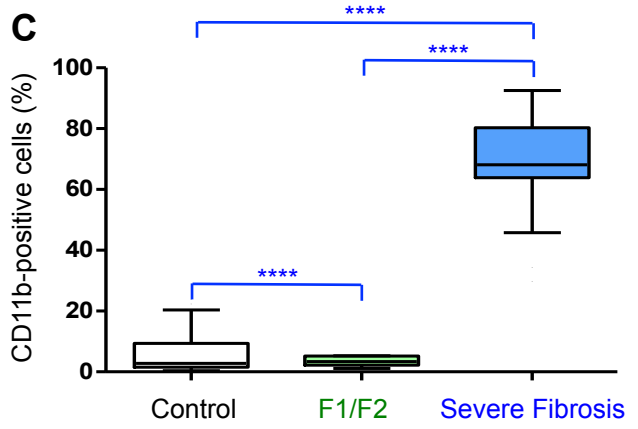

Figure S16. The number of CD11b-positive cells increases in patients with severe fibrosis. Human liver samples from 6 controls (C1 to C6, Stage F0), a patient diagnosed with stage F1/F2 (P1) and 4 patients (P2 to P5) diagnosed with severe liver fibrosis (≥ F3) were stained with anti-CD11b antibody. **(A)** Quantification of CD11b-positive cells (%) from each sample (of at least 5 areas per sample). Boxplots with whiskers indicate the Least Square Mean (LSM), including maximum and minimum values and the median value of the data set. **(B)** LSM test was used to analyze the mean difference between any pair of subjects without multiplicity adjustments. Table represents *p-values* between any pair of subjects. A *p*-value, less than 0.05, was considered to be statistically significant. **(C)** One-way ANOVA was used to test the mean between control group, F1/F2 patient and severe fibrosis group. Pair-wise comparisons indicated a *p-value* <0.0001 between any pair of groups.

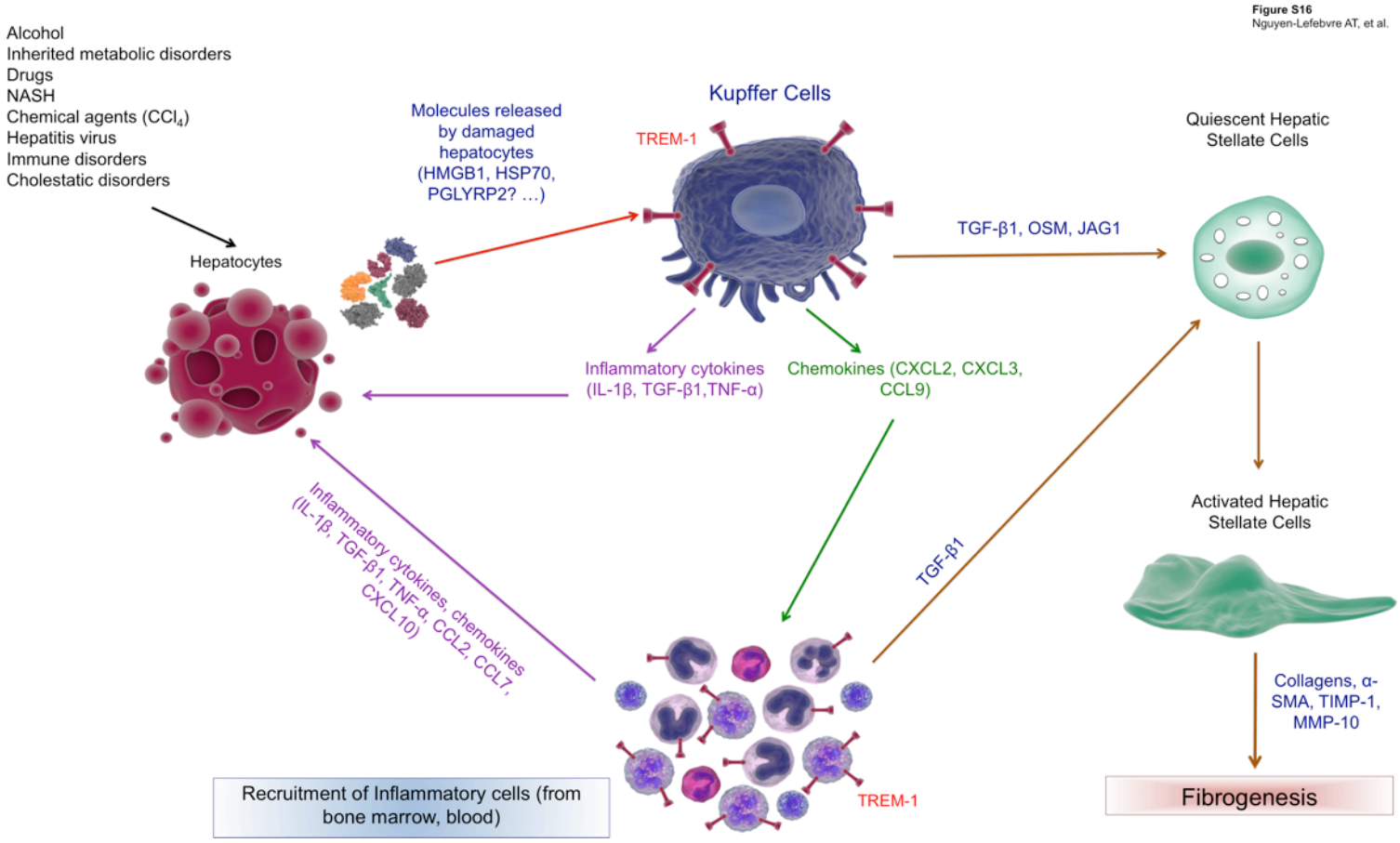

Figure S17. Role of TREM-1 on Kupffer cells in liver fibrogenesis. CCl_4 specifically targets hepatocytes, inducing hepatocellular injury through its metabolites (black arrow). Damaged hepatocytes release various molecules, including HMGB1, HSP70, and PGLYRP1, that bind to TREM-1 on Kupffer cells and activate them (red arrow). Activated Kupffer cells produce multiple chemokines (e.g., CXCL3, CCL9, and CXCL2) (green arrow) that initiate and maintain the recruitment of inflammatory cells from bone marrow and blood to injured liver. Kupffer cells activate HSCs *via* TGF-β1, OSM and JAG1 (brown arrows). Recruited cells activate HSCs *via* TGF-β1 (brown arrows). Activated HSCs induce liver fibrogenesis. Kupffer cells and recruited inflammatory cells secrete important cytokines (purple arrows), including TNF-α, TGF-β1 and IL-1β, thereby further enhancing hepatocyte damage.

Supplemental Table 1: Primer sequences used for PCR and RT-qPCR and the expected product size.

Gene		Sequence of primers	Product size
Col1a1	Forward	5' CAGTCGATTCACCTACAGCACG 3'	201 bp
	Reverse	5' GGGATGGAGGGAGTTTACACG 3'	
Col1a2	Forward	5' CTGCTCAGTATTCTGACAAAGGAG 3'	87 bp
	Reverse	5' CTCCAACAGCACCAGGAG 3'	
Col3a1	Forward	5' CTGGAGAACCTGGTGCAAAT 3'	67 bp
	Reverse	5' CCTCGGAAGCCACTAGGAC 3'	
Col4a1	Forward	5' GCGAAGGGCGATTGTGGT 3'	89 bp
	Reverse	5' AACCCTGGCAAGCCTCTTTC 3'	
Col5a1	Forward	5' AAGCGTGGGAAACTGCTCTCCTAT 3'	118 bp
	Reverse	5' AGCAGTTGTAGGTGACGTTCTGGT 3'	
Tgfb1	Forward	5' TGGAGCAACATGTGGAACTC 3'	73 bp
	Reverse	5' GTCAGCAGCCGGTTACCA 3'	
Acta2	Forward	5' ATCGTCCACCGCAAATGC 3'	90 bp
	Reverse	5' AAGGAACTGGAGGCGCTG 3'	
Mmp10	Forward	5' CCTGATGTTGGTGGCTTCAGT 3'	86 bp
	Reverse	5' CTGGTGTATAATTCAATCCTGTAGGT 3'	
Edn1	Forward	5' CCTGGACATCATCTGGGTC 3'	109 bp
	Reverse	5' TGTGGCCTTATTGGGAAG 3'	
Birc5	Forward	5' ATCCACTGCCCTACCGAGAA 3'	201 bp
	Reverse	5' CTTGGCTCTCTGTCTGTCCAGTT 3'	
Timp1	Forward	5' AGGTGGTCTCGTTGATTTCT 3'	108 bp
	Reverse	5' GTAAGGCCTGTAGCTGTGCC 3'	
Hhip	Forward	5' TGCCACCAACAACTCAGAATG 3'	119 bp
	Reverse	5' CTAGGTCCCCATCCAGGACA 3'	
Plxnc1	Forward	5' CAGAGACGCCAATGACAAGA 3'	227 bp
	Reverse	5' TACTGCACTGCTCCATCAGG 3'	
Trem1	Forward	5' CGCCTGGTGGTGACCAAGGG 3'	152 bp
	Reverse	5' ACAACCGCAGTGGGCTTGGG 3'	
Ccl2	Forward	5' GTTGGCTCAGCCAGATGCA 3'	81 bp
	Reverse	5' AGCCTACTCATTGGGATCATCTTG 3'	
Ccl7	Forward	5' CCAATGCATCCACATGCTGC 3'	100 bp
	Reverse	5' GCTTCCCAGGGACACCGAC 3'	
Cxcl10	Forward	5' CGATGGATGGACAGCAGAGAGCC 3'	147 bp
	Reverse	5' CCATGGCTTGACCATCATCCTGCAG 3'	
Tnf-α	Forward	5' GCCTCTTCTCATTCCTGCTTG 3'	115 bp
	Reverse	5' CTGATGAGAGGGAGGCCATT 3'	
Il-1b	Forward	5' TGTAATGAAAGACGGCACACC 3'	68 bp
	Reverse	5' TCTTCTTTGGGTATTGCTTGG 3'	
Il-6	Forward	5' CAAAGCCAGAGTCCTTCAGA 3'	102 bp
	Reverse	5' GATGGTCTTGGTCCTTAGCC 3'	
Actb	Forward	5' AGATGACCCAGATCATGTTTGAGA 3'	65 bp
	Reverse	5' CACAGCCTGGATGGCTACGT 3'	
rRNA 18S	Forward	5' ATGGTAGTCGCCGTGCCTAC 3'	62 bp
	Reverse	5' CCGGAATCGAACCCTGATT 3'	
Gapdh	Forward	5' GGTGAAGGTCGGTGTGAACG 3'	233 bp
	Reverse	5' CTCGCTCCTGGAAGATGGTG 3'	
Hrpt1	Forward	5' CAGTCCCAGCGTCGTGATTA 3'	167 bp
	Reverse	5' GGCCTCCCATCTCCTTCATG 3'	

Supplemental references

1. Pfaffl MW. A new mathematical model for relative quantification in real-time RT-PCR. *Nucleic acids research.* 2001;29(9):e45.
2. Bolger AM, Lohse M, and Usadel B. Trimmomatic: a flexible trimmer for Illumina sequence data. *Bioinformatics.* 2014;30(15):2114-20.
3. Dobin A, Davis CA, Schlesinger F, Drenkow J, Zaleski C, Jha S, Batut P, Chaisson M, and Gingeras TR. STAR: ultrafast universal RNA-seq aligner. *Bioinformatics.* 2013;29(1):15-21.

Full unedited gel for Figure 1F

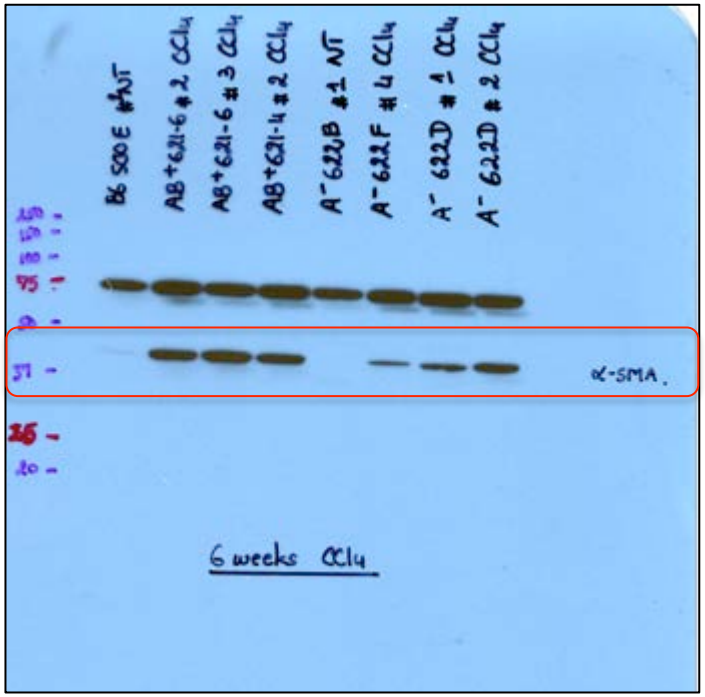

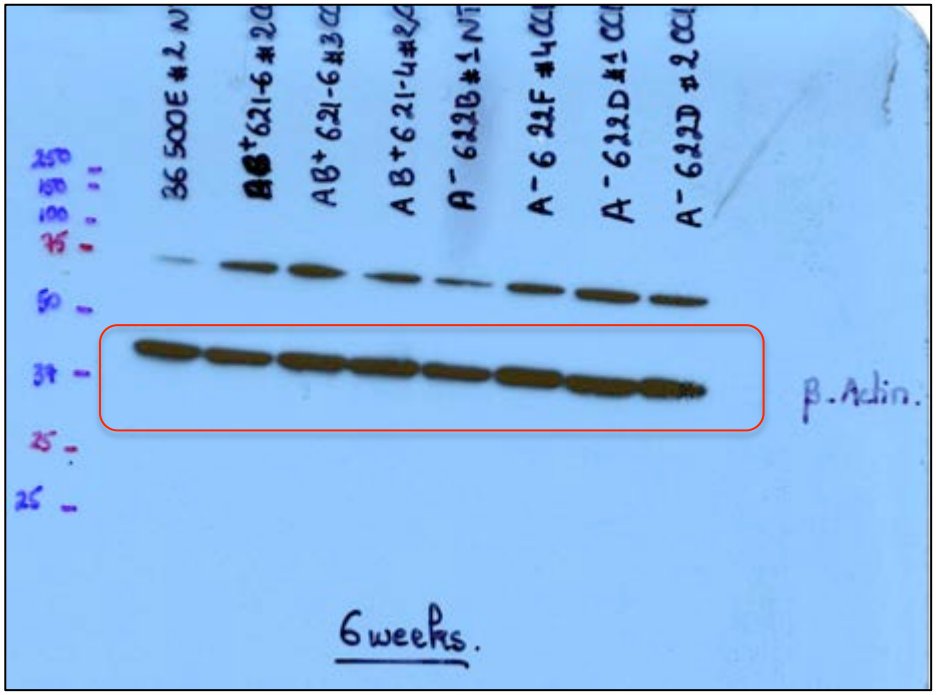

Full unedited gel for Figure 6B

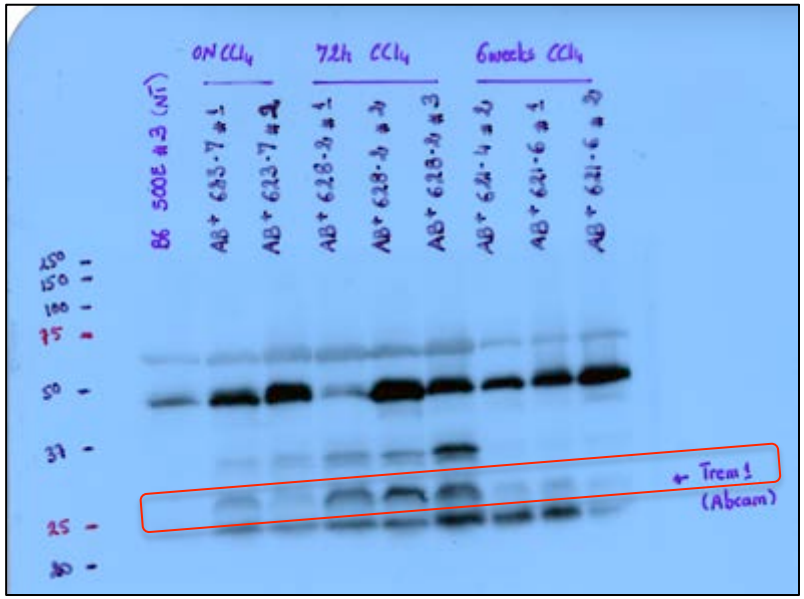

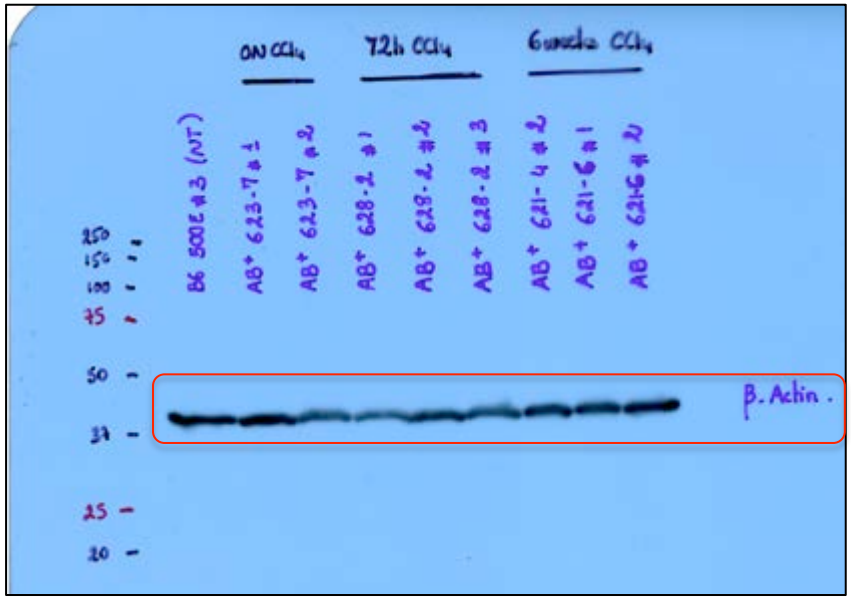

Full unedited gel for Supplemental Figure 9A

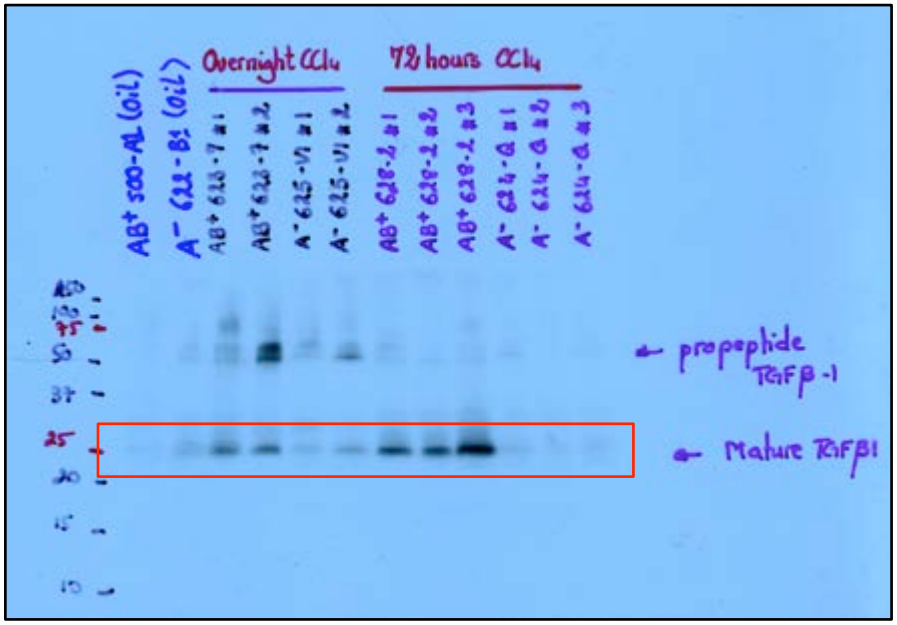

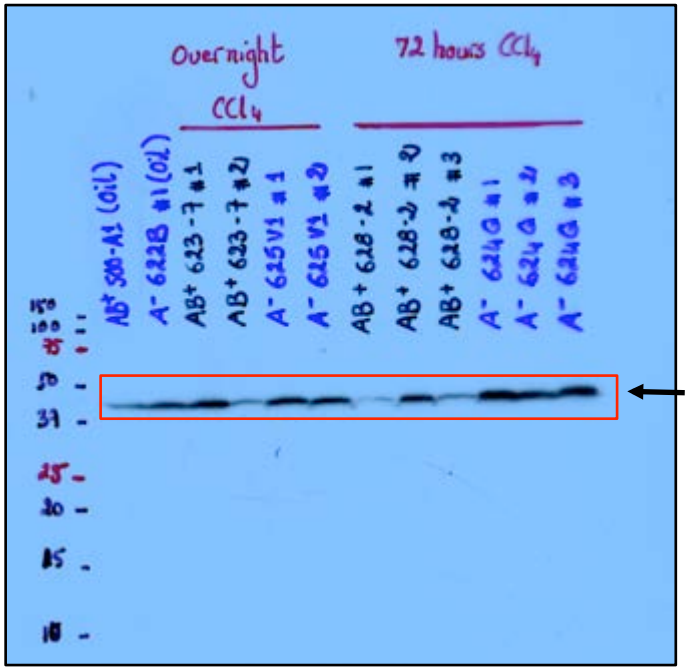

Full unedited gel for Figure 6E